LINEAR INVERTED PENDULUM MODEL AND SWING LEG DYNAMICS IN BIPED ROBOT WALKING TRAJECTORY GENERATION

by
UTKU SEVEN

Submitted to the Graduate School of Engineering and Natural Sciences
in partial fulfillment of
the requirements for the degree of
Master of Science

Sabanci University
July 2007

LINEAR INVERTED PENDULUM MODEL AND SWING LEG DYNAMICS IN BIPED ROBOT WALKING TRAJECTORY GENERATION

APPROVED BY:

Assist. Prof. Dr. Kemalettin ERBATUR
(Thesis Advisor) ……..

Prof. Dr. Asif. ŞABANOVİÇ ……..

Assoc. Prof. Dr. Mustafa ÜNEL ……...

Assist. Prof. Dr. Ahmet ONAT ……...

Assist. Prof. Dr. Albert LEVI ……..

DATE OF APPROVAL: ……..

LINEAR INVERTED PENDULUM MODEL AND SWING LEG DYNAMICS IN BIPED ROBOT WALKING TRAJECTORY GENERATION

Utku SEVEN

EECS, Ms Thesis, 2007

Thesis Supervisor: Assist. Prof. Dr. Kemalettin ERBATUR

Keywords: Linear Inverted Pendulum Model, Zero Moment Point, state-space representation, swing leg gravity compensation

ABSTRACT

Expectations of people and researchers from robotics have changed in the last four decades. Although robots are used to play their roles in the industrial environment, they are anticipated to meet social demands of people in daily life. Therefore, the interest in humanoid robotics has been increasing day by day. Their use for elderly care, human assistance, rescue, hospital attendance and many other purposes is suggested due to their adaptability and human like structure.

Biped reference trajectory generation is a challenging task as well as control owing to the instability trend, non-linear robot dynamics and high number of degrees of freedom. Hence, the generated reference trajectories have to be followed with minimum control interference. Linear Inverted Pendulum Model (LIPM) is used to meet this demand which assumes the body as a falling point mass connected to the ground with a massless rod. The Zero Moment Point (ZMP) is a stability criterion for legged robots which provides a more powerful, stable reference generation. With the assistance of this methodology, advanced Linear Inverted Pendulum Models are implemented.

This thesis aims to improve the applicability of the versatile and computationally effective LIPM based reference generation approach for the robots with heavy legs. It proposes a swing-leg gravity compensation technique based on a two-mass linear inverted pendulum model which is simulated on a discrete state space model. LIPM modeling is implemented by switching between one-mass and two-mass models during double support and single support phases, respectively. The joint trajectories are then obtained by inverse kinematics and PID controllers are employed independently at joint level for locomotion.

The effectiveness of the generated reference trajectories is verified by simulation. The reference generation and control algorithm is tested with a 3-D full dynamic simulator on the model of a 12 DOF biped robot. Results indicate better performance of the one-mass-two-mass switching LIPM over the one-mass LIPM.

DOĞRUSAL TERS SARKAÇ MODELİ VE İKİ BACAKLI YÜRÜYEN ROBOTLARDA YÖRÜNGE ELDE EDİLMESİNDE SALINAN BACAK DİNAMİĞİ

Utku SEVEN

EECS, Master Tezi, 2007

Tez Danışmanı: Yrd. Doç. Dr. Kemalettin ERBATUR

Anahtar Kelimeler: Doğrusal Ters Sarkaç Modeli, Sıfır Moment Noktası, durum-uzay gösterimi, salınan bacak yer çekimi telafisi

ÖZET

Son kırk yılda insanların ve araştırmacıların robotik biliminden beklentilerinde bir değişim olduğu görülmüştür. Robotların endüstrideki yerini göz önünde bulundurmakla beraber, insanların günlük hayatlarındaki isteklerini karşılamaları da beklenmektedir. Bu sebepten insansı robotlara olan ilgi gün ve gün artış göstermektedir. İnsanların yaşadığı ortamlar uyum sağlamaları ve insana benzer yapıları sebebiyle kurtarma çalışmaları, hasta bakıcılığı ve asistanlık gibi görevleri üstlenmeleri istenmektedir.

Fakat lineer olmayan karasız dinamikleri ve çok sayıda eklemleri yüzünden kontrol edilmeleri çok zorlu bir görev olmakla beraber bu robotlar için yürüyüş referansı elde edimi de çok zordur. Bu yüzden yaratılan referansların izlenmesi için çok fazla kontrol müdahalesi gerekmemesi istenmektedir. Lineer Ters Sarkaç Modeli (LIPM) böyle referansların elde edilmesi için uygun bir altyapı sağlamaktadır. Bu modelde vücut bir noktasal ağırlık olarak kabul edilmekle beraber bacaklar da ağırlıksız çubuklar olarak modellenmektedir. Buna ek olarak Sıfır Moment Noktası (ZMP) da kararlı referans elde edilmesi için güçlü bir yöntem olmakla beraber robotun kararlılığı açısından çok önemli bir kriterdir. Bu kriter yardımıyla gelişmiş Lineer Ters Sarkaç Modelleri elde edilmiş ve uygulanmıştır.

Bu tezin amacı ağır bacaklı robotlar için LIPM tabanlı, işlemsel uygulama açısından avantajlı olan ve çok yönlü bir referans oluşturma tekniği geliştirmektir. Bunun için ayrık zamanlı durum-uzay modellerine sahip çift noktasal ağırlık içeren bir LIPM modeli önermektedir. LIPM modeli uygulaması tek ayak destek ve çift ayak destek safhalarına göre sırasıyla tek ve çift noktasal ağırlıklı modeller arasında geçiş yardımıyla elde edilmiştir. Elde edilen referanstan ters kinematik yardımıyla eklem değişkenleri elde edilmiş ve her eklem için bağımsız PID denetleyicileri kullanılmıştır.

Yaratılan referansın verimi benzetim yardımıyla doğrulanmıştır. Benzetim, bu referansların 12 serbestlik dereceli bir robotun 3B dinamik modeline uygulanması ile gerçekleştirilmiştir. Elde edilen sonuçlar kullanılan modelin tek ağırlıklı modele göre daha iyi sonuçlar verdiğini doğrulamaktadır.

To my family

ACKNOWLEDGEMENTS

It is a pleasure to thank the many people who made this thesis possible.

It is difficult to overstate my gratitude to my MS. supervisor, Asst. Prof. Dr. Kemalettin ERBATUR. With his enthusiasm, his inspiration, and his great efforts to explain things clearly and simply, he made this thesis possible with the highest priority. Throughout my thesis-writing period, he provided encouragement, sound advice, good teaching, good company, and lots of good ideas. I would have been lost without him. I would like to express my deepest regards and appreciation to Assoc. Prof. Dr. Mustafa Ünel and Asst. Prof Dr. Güllü Kızıltaş Şendur for their invaluable support for the realization of my thesis.

I am indebted to my many student colleagues for providing a stimulating and fun environment in which to learn and grow. I am especially grateful to Berk Çallı, Erol Özgür, Yeşim Hümay Esin, Hakan Bilen, Meltem Elitaş, Nusrettin Güleç, Emrah Deniz Kunt, Teoman Naskali and many other friends in Sabancı University mechatronics laboratories.

Lastly, and most importantly, I wish to thank my parents, Ayşe Seven and Nedim Seven, my brother Özgür Seven and his wife Ipek Seven. They bore me, raised me, supported me, taught me, and loved me. To them I dedicate this thesis.

LINEAR INVERTED PENDULUM MODEL AND SWING LEG DYNAMICS IN BIPED ROBOT WALKING TRAJECTORY GENERATION

TABLE OF CONTENTS

LIST OF FIGURES

LIST OF TABLES

LIST OF SYMBOLS

$\boldsymbol{A}_B$	:	Base-link attitude matrix
$\boldsymbol{C}(\boldsymbol{x},\boldsymbol{v})$	:	Centrifugal and Corioli's force matrix
$\boldsymbol{f}_E$	:	External force vector
$\boldsymbol{g}(\boldsymbol{x})$	:	Gravity vector
$\boldsymbol{H}(\boldsymbol{x})$	:	Inertia matrix
K_d	:	PID controller derivative gain
K_i	:	PID controller integral gain
K_p	:	PID controller proportional gain
$\boldsymbol{u}_E$	:	Generalized force vector generated by external forces
$\boldsymbol{v}$	:	Generalized velocities vector
$\boldsymbol{v}_B$	:	Base-link velocity vector
$\dot{\boldsymbol{v}}_B$	:	Base-link acceleration vector
$\boldsymbol{w}_B$	:	Base-link angular velocity vector
$\dot{\boldsymbol{w}}_B$	:	Base-link angular acceleration vector
$\boldsymbol{\theta}$	:	Joint angle vector
x_{ZMP}	:	Zero Moment Point in x-direction
y_{ZMP}	:	Zero Moment Point in y-direction
P	:	Zero Moment Point reference vector
c_z	:	Constant height of the Linear Inverted Pendulum
ω	:	Square root of c_z / g
P_x^{ref}	:	Reference ZMP for x-direction
P_y^{ref}	:	Reference ZMP for y-direction
A	:	Foot center to foot center distance in frontal plane
B	:	Foot center to foot center distance in saggittal plane
T_0	:	Step Period
b	:	Half length of the foot sole

$T_{L_0}^{L_6}$: Transformation matrix bringing the foot coordinates to the hip coordinates for the left leg

q_L : Joint variable vector for left leg

$A_{L_0}^{L_6}$: Rotation matrix bringing the foot coordinates to the hip coordinates for the left leg

$d_{L_0}^{L_6}$: The vector distance between the hip and the foot of the left leg

$\ddot{c}_x$: x-directional acceleration of the robot body

c_x : x-directional position of the robot body

c_z : z-directional position of the robot body

$\ddot{c}_y$: y-directional acceleration of the robot body

c_y : y-directional position of the robot body

$\ddot{l}_x$: x-directional acceleration of the swing leg

l_x : x-directional position of the swing leg

l_z : z-directional position of the swing leg

$\ddot{l}_y$: y-directional acceleration of the swing leg

l_y : y-directional position of the swing leg

γ : Square root of l_z / g

M : Mass of whole robot

m : Mass of swing leg

LIST OF ABBREVIATIONS

COM	:	Center of Mass
CMB	:	Center of Mass of Body
CML	:	Center of Mass of Swing Leg
ZMP	:	Zero Moment Point
PID	:	Proportional Integral
2-D	:	Two Dimensional
3-D	:	Three Dimensional
LIPM	:	Linear Inverted Pendulum Mode
D.O.F	:	Degrees of Freedom
LxWxH	:	Length x Width x Height
DH	:	Denavit Hartenberg

Chapter 1

INTRODUCTION

Expectations of people and researchers from robotics have changed in the last four decades. Robots used to play their roles in industrial environments as automation apparatus for people. In addition to this, they are starting to fulfill responsibilities in our daily environments like hospitals, homes and offices in recent years. Therefore, the interest in humanoid robotics has been increasing day by day. Humanoid robots can be regarded as assistants for humans. Their use for elderly care, human assistance, rescue, hospital attendance and many other purposes is suggested. The adaptability of the anthropomorphic structure to the human environment is one of the reasons of this interest.

When compared to wheeled or other multi legged robots (quadropedal, six legged, eight legged etc.), it can be easily realized that bipedal humanoid robot is a more proper choice for social interaction. Wheeled robots are considered to serve better on smooth surfaces due to their ground contact geometry. But human environment generally does not consist of smooth ground surfaces. Hence the mobility of wheeled robots in human environment is limited. Furthermore, other multi legged robots can adapt to rugged terrain but may not be conformable for human interaction such as elderly care, hospital attendance or baby sitting due to their shape and appearance.

In addition to this, bipedal locomotion is capable of mimicking all human-actions theoretically. Using this ability, humanoid robots are supposed to work under tough environmental conditions such as radioactive environments, fire rescue and space applications.

Biped reference trajectory generation is a challenging task. Due to the instability, non-linear robot dynamics and high number of degrees of freedom, control is also a difficult

problem. Hence, the generated reference trajectories have to be followed with minimum control interference. Linear Inverted Pendulum Model (LIPM) is used to meet this demand. In Linear Inverted Pendulum Model, the humanoid robot is considered as a single point mass and supporting legs are modeled as massless rods. According to this model body starts to fall through the walking direction. Before falling completely, supporting leg changes and the walking cycle is obtained using this sequence. In this model, the height of the point mass is assumed to be constant. With this assumption, the model becomes linear and decoupled in horizontal directions.

The Zero Moment Point (ZMP), introduced by Vukobratovich is used as a stability criterion for legged robots. Usage of this criterion provides a more powerful and stable reference generation approach with the Linear Inverted Pendulum Model. With the assistance of this methodology, advanced Linear Inverted Pendulum Models are implemented.

In many projects around the globe, successful results are obtained. However there is a problem associated with the LIPM: LIPM assumes that the robot body can be modeled as a single point mass and the legs as massless rods although they have considerable masses. This causes disturbing gravity effects of the swing leg to be more pronounced and makes the control task more difficult, especially for robots with heavy legs. Heavy legged structures are quite common due to the high torque requirements and many (usually six) degrees of freedom required to mimic human dexterity. A number of electrical motors and reduction mechanisms are usually employed in the leg structures

This thesis aims to improve the applicability of the versatile and computational effective LIPM based reference generation approach for the robots with heavy legs.

It proposes a swing-leg gravity compensation technique which is based on a two-mass inverted pendulum model. In this approach swing leg reference trajectory generation is realized by using swing-leg center of mass positions (CML – Center of Mass of Leg) and body center of mass positions (CMB – Center of Mass of Body). The reference CMB positions are obtained offline, by simulations on a discrete state space model of the LIPM.

LIPM modeling is implemented by switching between one-mass and two-mass models during double support and single support phases, respectively. Two different discrete state space models are obtained for single support and double support phases. In single support

phase, the LIPM used consists of two point masses. One of them is the sum of trunk (robot body) and the support leg, the other one is the mass of swing leg. In double support phase, our model includes one mass that consists of the mass of trunk and two legs together. The one-mass model is described by a third order state-space realizations and a fifth order state-space system is used to describe the dynamics of the two-mass model in both realizations, the CMB is one of the state variables. Simulating the state-space model under state feedback to reach desired ZMP and swing foot trajectories, and recording the CMB history provides the CMB reference. The joint trajectories are then obtained by inverse kinematics and PID controllers are employed independently at joint level for locomotion.

The effectiveness of the generated reference trajectories is verified by simulation. The reference generation and control algorithm is tested with a 3-D full dynamic simulator on the model of a 12 DOF biped robot. Results indicate better performance of the one-mass-two-mass switching LIPM over the one-mass LIPM.

Chapter 2 presents a literature survey on reference generation methods, successful examples of humanoid robots in the world, gravity compensation methods and their applications to the real robots. Chapter 3 represents the bipedal humanoid robot model and mechanical design parameters. Linear Inverted Pendulum Model, its state space model and reference trajectory generation by a swing leg gravity compensation method is introduced in various scenarios in Chapter 4. Chapter 5 includes locomotion control algorithms. Chapter 6 includes simulation results and finally conclusions and future works are presented in Chapter 7.

Chapter 2

2. LITERATURE REVIEW

In this chapter a literature review on biped walking robot research is presented. The review begins in the next section with an introduction of terminology. Successful biped robot projects are reviewed in Section 2.2. Section 2.3 discusses main approaches in on walking reference generation.

2.1. Humanoid Locomotion Terminology

Humankind got used to walk in their early ages and start to walk on rugged terrain, climb a wall or run. This shows that humans are successful walking beings. These locomotions are admitted as simple movements even though it is very difficult to obtain these motions successfully for humanoid robots. These motions are separated and examined for different reference planes in humanoid robotics. These reference planes are shown in Figure 2.1 [1]

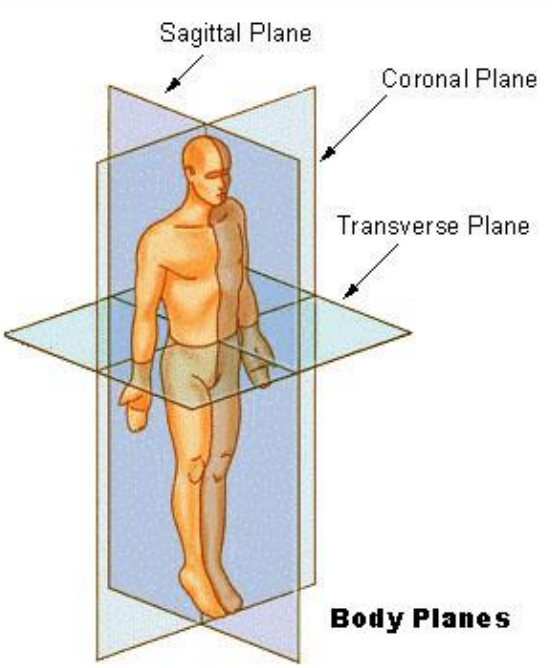

Figure 2.1 Reference body planes

These reference planes are very important to analyze walking locomotion. For simplification purpose, only walking through saggital plane is considered in some studies [2].

The supporting polygon is defined as the polygon shaped area which is determined between the foot corners that are touching the ground. This area is described differently in various phases of walking locomotion as seen in Figure 2.3 [3].

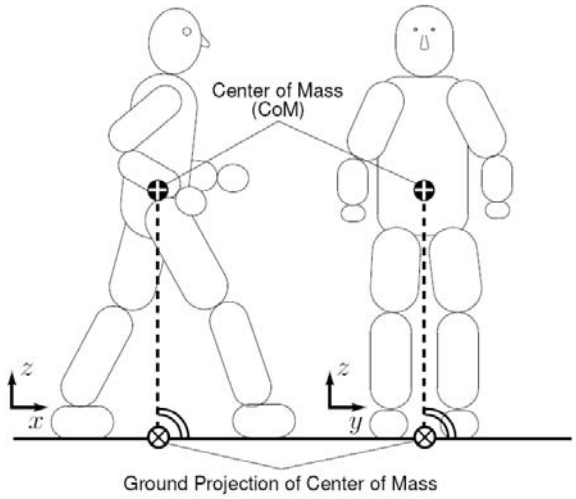

Figure 2.2 COM and Ground Projection

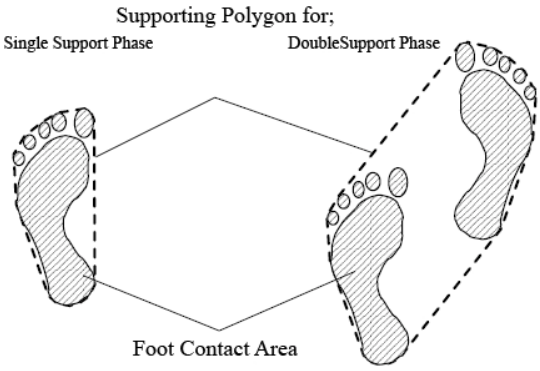

Figure 2.3 Supporting Polygon

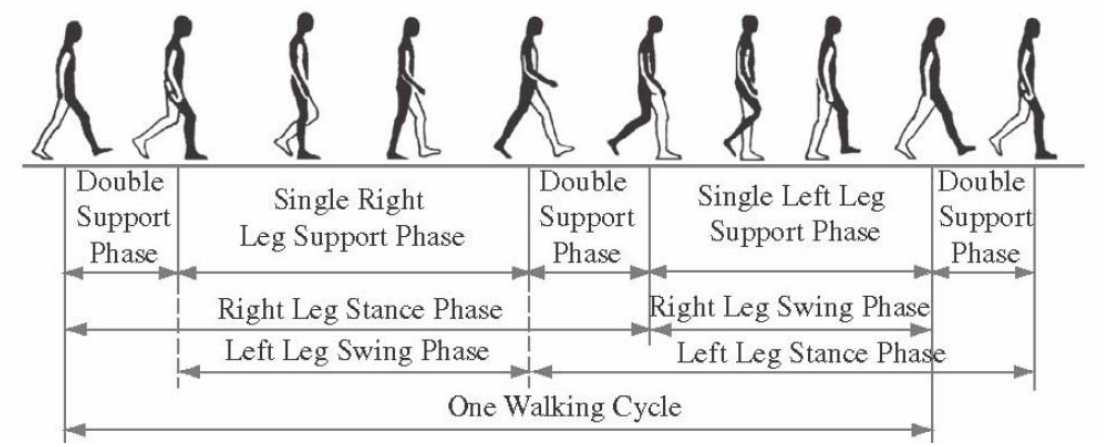

Figure 2.4 Walking Locomotion

Walking can be separated into two different phases [4]. The single-support phase is the phase in which only one foot is in contact with the ground. In the double-support phase both feet are on the ground. During the single-support phase the foot in contact with the ground is called stance or support foot and the other one is called the swing foot. Support foot's position is of primary importance for the stability. These phases are shown in Figure 2.4 [5].

Walking can be analyzed in different categories. One of them is static walking locomotion that generates static gait (Figure 2.5), which occurs at low speeds. The ground projection of robot center of mass (COM) position is kept in supporting polygon in both single and double support phases.

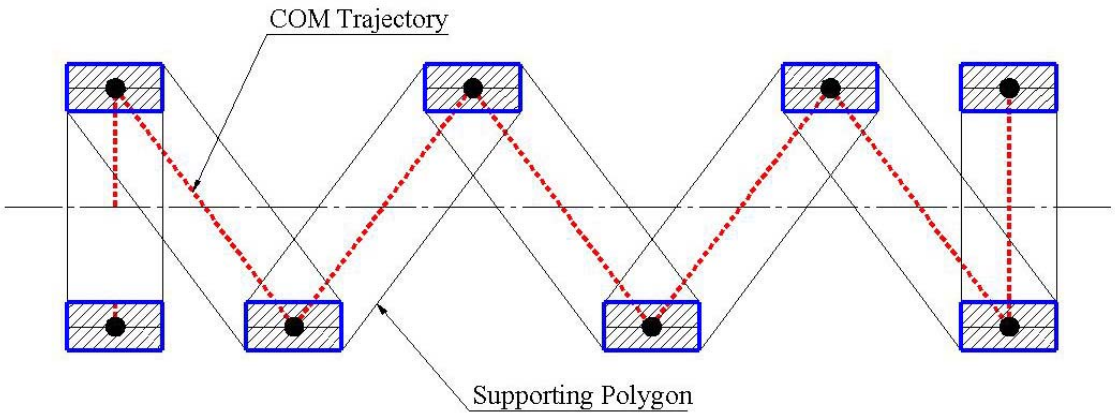

Figure 2.5 Static Walking Gait and COM Trajectory

Another category is dynamic walking. In this kind of walk the COM projection leaves the supporting polygon. This is a mode difficult to achieve type of walking and humans usually walk in this mode.

Step length and stride length are important parameters that affect the stability of the walk. The step length can be defined as the additional distance traveled by one foot to the previous one, and the stride length is the distance between two successful positions of the same foot.

The ZMP Criterion [6, 7] introduced to the robotics literature in early 1970s is widely employed in the stability analysis of legged robot locomotion. It can be described as the point on the ground where the tipping moment acting on the biped, due to gravity and inertia forces, equals zero. The tipping moment is defined as the component of the moment that is tangential to the supporting surface [8]. The location of the ZMP in the supporting polygon can be used as a measure of the stability of the robot: If it is close to the boundary of the supporting polygon, the robot is considered to be close to a tip over at this boundary location, typically at an edge of a supporting foot.

2.2. History of Humanoid Walking Robots

The curiosity of humankind on its locomotion has started the study of biomechanics and motion. This curiosity has its roots in early ages. Plato wrote:

In order then that it might not tumble about among the high and deep places of the earth, but might be able to get over the one and out of the other, they provided the body to be its vehicle and means of locomotion; which consequently had length and was furnished with four limbs extended and flexible; these God contrived to be instruments of locomotion with which it might take hold and find support, and so be able to pass through all places, carrying on high the dwelling place of the most sacred and divine part of us. Such was the origin of legs and hands, which for this reason were attached to every man. [9]

Timaeus (360 BC) by PLATO, translated by Benjamin

Figure 2.6 shows an engraving by Giovanni Alfonso Borelli 1608-79, another scientist who worked to understand humans and animals in terms of mathematics and equations. Borelli was an Italian physiologist, physicist, astronomer, and mathematician who studied the mechanics and dynamics of organic motion.

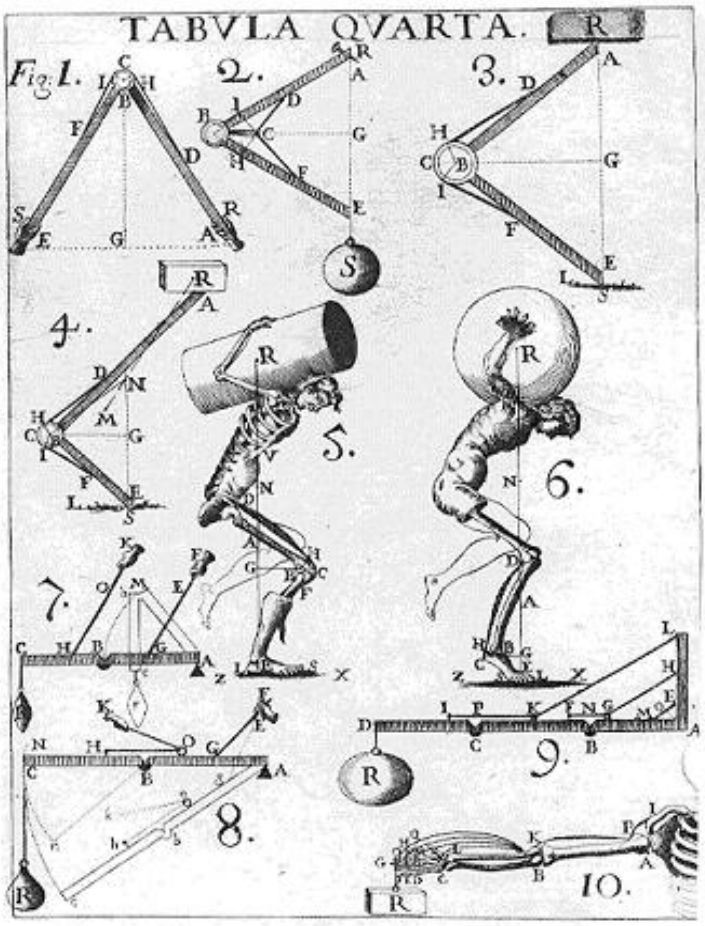

Figure 2.6 An engraving by Giovanni Alfonso Borelli

In the beginning of the second half of the 20th Century, age of humanoid robots have grown and many researchers started to build successful examples of bipedal walking robots [10, 11, 12, 13]. The first computer controlled humanoid robot was built at the WASEDA University in 1967 by Bio-engineering Group, which was called WABOT-I [14]. The WABOT-1 was able to communicate-with a person in Japanese and to measure distances and directions to the objects using external receptors, artificial ears and eyes, and an artificial mouth. The WABOT-1 walked with his lower limbs and was able to grip and transport objects with hands that used tactile-sensors. After this considerable step in humanoid robotics world, many other robots are built. Waseda University Bio-Engineering Group continued its work with WHL-11, WL-5, WL-9DR and WL-10. During this period M.H. Raibert's hopping machine [15] was introduced and ballistic flight phase was added to the humanoid robotics literature (Figure 2.7).

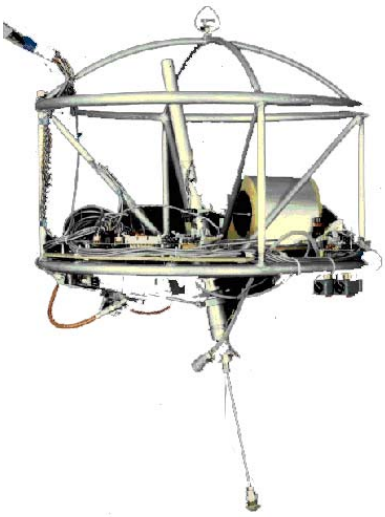

Figure 2.7 Raibert's Hopping Machine

After those approaches full sized, more human-like humanoid robots were built. A successful example of them is WABIAN-2 of Waseda University (Figure 2.8). This humanoid robot is built to propose the efficiency of humanoid robot as a type of robot to work in human environment [16, 17]. It is expected to cooperate with human due to its affinity, isomorphism and adaptability to human environment. WABIAN-2 is 1530 [mm] height and 512 [mm] width respectively, and has 41 D.O.F.

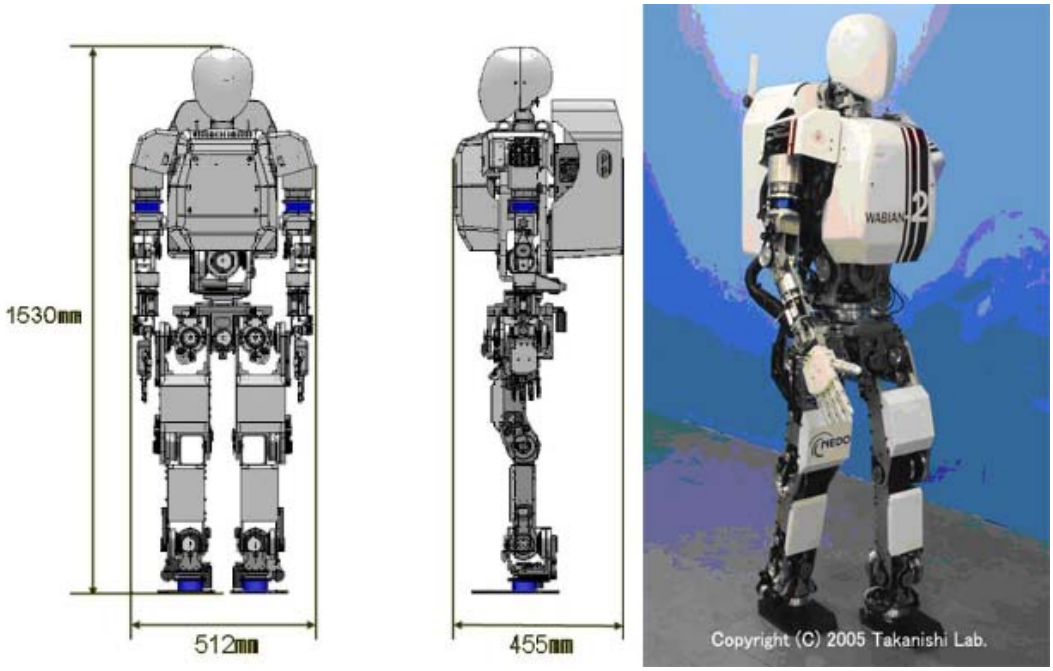

Figure 2.8 WABIAN-2 of Waseda University

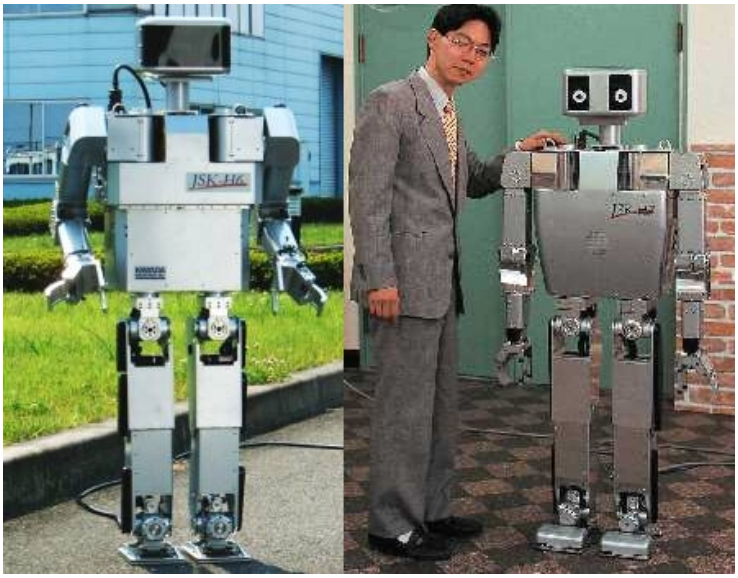

Figure 2.9 H6 (on the left side) and H7 (on the right side) of University of Tokyo

Furthermore, University of Tokyo constructed H6 and H7 humanoid robots [18]. H6 is 1370 [mm] height and 590 [mm] width respectively, and has a total of 35 D.O.F. Its weight is 55 [kg]. H6 is light weighted despite its human size dimensions. Aircraft technology is utilized for body parts. H6 and H7 can walk up and down 25 [cm] high steps and can also recognize pre-entered human faces (Figure 2.9).

On the other hand European universities have successful research results like JOHNNIE [19]. It is constructed by Technical University of Munich for the realization of dynamically three-dimensional walking and jogging motion. It has an anthropomorphic biped robot structure that allows adaptability to human environment. Johnnie acquires a highly developed vision control capability [3]. It can recognize obstacles by stereo camera vision technology. Johnnie classifies obstacles and plans a suitable trajectory that can even able to step over the obstacle. Thus the robot is able to handle obstacles without stopping walking locomotion and shows a very smooth walking performance when a suitable walking trajectory is found.

KHR-2 of Korea Advanced Institute of Science and Technology with 41 D.O.F. is another successful example that is capable of human-robot interaction, AI (Artificial Intelligence), visual & image recognition and navigation [20] (Figure 2.10).

Figure 2.10 KHR-2 of Korea Advanced Institute of Science and Technology

A small size humanoid robot PINO is constructed and developed by Japan Science and Technology Corporation, ERATO to realize a compact, low-priced, expansible and mobile humanoid robot [21]. It is 70 [cm] tall, which is the size of a one year old child. It has a total of 26 D.O.F. It is capable of keeping its body's balance, moving the swing leg, operating a grasping object and controlling visual attention (Figure 2.11).

Another compact size humanoid robot is SDR-3X (Sony Dream Robot-3X) [22]. The concept of this small size robot does not follow the idea of a universal helper, but is rather designed as an entertainment platform [23]. Its specifications are 500 [mm] height, 220 [mm] width, 5 [kg] weight, and 24 D.O.F. SDR-3X can more than just walk around such as squatting, getting up, and doing synchronized choreography, though it can't go up and down stairs since Sony developed it for entertainment (Figure 2.11). SDR-3X has a highly advanced equilibrium system allowing it to balance on a moving surf board or skating on roller skates. As a new contribution to literature SDR-3X utilizes a new tool that allows people teach new motion algorithms to the SDR-3X humanoid robot. This can be used for even external forces so that the robot can grab a ball and throw it out. Sony’s SDR-4X and QRIO models followed this robot with increased walking speed.

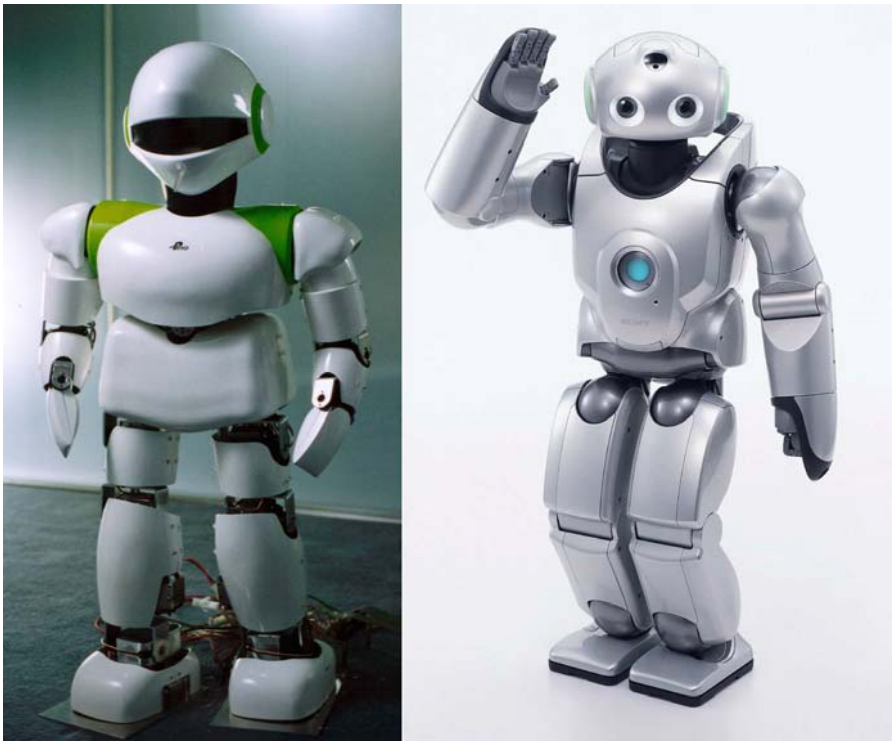

Figure 2.11 PINO (on the left side) and Sony SDR 3X (on the right side)

HONDA Company has developed the most impressive and the most attractive humanoid robots and received the world's humanoid research communities attention and excitement (Figure 2.12). P2, the second prototype HONDA humanoid robot, was revealed in 1996 after ten years of secret research. With this new born humanoid innovation, the robotics world was stunned. P2 can walk and go up and down stairs.

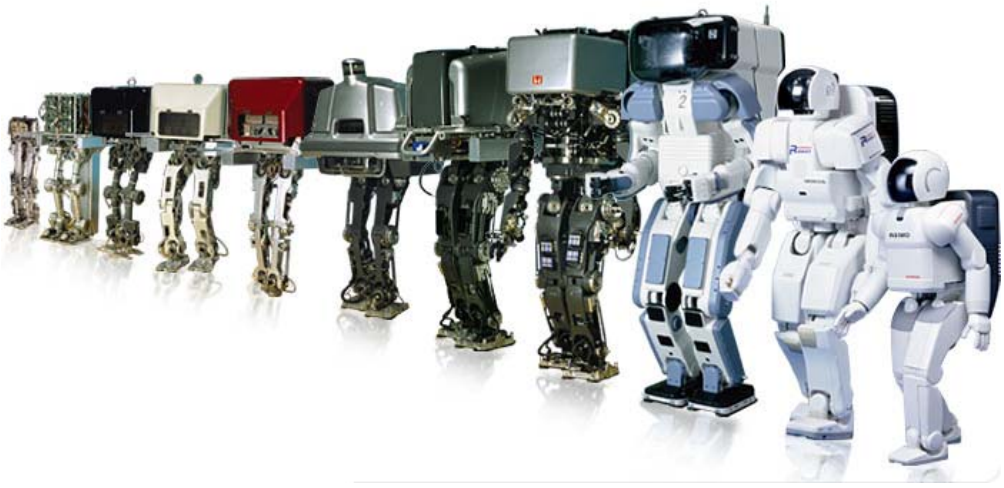

Figure 2.12 HONDA Humanoid Robots

Figure 2.13 ASIMO of HONDA Company

Downsizing P2 (1820 [mm] height, 600 [mm] width, 210 [kg] weight including batteries, 6 D.O.F./Leg, 7 D.O.F./Arm, 2 D.O.F./Hand), P3 (1600 [mm] height, 600 [mm] width, 130 [kg] weight including batteries, 6 D.O.F./Leg, **7** D.O.F./Arm, 1 D.O.F./Hand) appeared in 1997 with the same mobility as P2 [24]. In 2000, further downsizing P3, ASIMO (Advanced Step in Innovative MObility) that stands for Advanced Step in Innovative Mobility appeared with children-size (1200 [mm] height, 450 [mm] width, 43 [kg] weight including batteries, 6 D.O.F./Leg, 5 D.O.F./Arm, 1 D.O.F./Hand, 2 D.O.F./Head) and new walking technology (i–WALK) (Figure 2.13). I-WALK technology helps ASIMO to walk continuously while changing direction or handling an obstacle. With the contribution of HONDA Company researchers interest have been attracted by humanoid robotics area. The more humanoid robots which can walk and can go up and down stairs are developed, the more humanoid robots are expected to perform several application tasks in an actual human living environment. However the application area of humanoid robots has still limited to the amusement and the entertainment. For research and development of humanoid robot performing application tasks, Ministry of Economy, Trade and Industry (METI) of Japan has launched a humanoid robotics project (HRP–I). The project is run from 1998 to 2002 for five

years, consisting of phase one for the first two years and phase two for the last three years. In phase one (1998-1999), a humanoid robotics platform (HRP–I), a tele-existence cockpit to control humanoid robots, and an equivalent virtual robot including dynamic simulator were developed. In phase two (2000-2002), research and development are carried out on the applications of humanoid robots (maintenance tasks of industrial plants, human care, tele-operations of construction machines, security services of home and office, and cooperative works in the open air) using HRP-I [25]. Improvement and addition of elemental technologies are also carried out in phase two. HRP–2 has two great features, which are especially necessary for cooperative works between other humanoid robots in the open air (Figure 2.14). First of them is that the ability of the biped locomotion of HRP–2 is improved so that HRP–2 can handle rough terrain in the open air. The second is that HRP–2 is designed in order to avoid tipping over easily. During the second phase of HRP-2 project HRP-3P was also being developed as an addition to this project [26]. HRP-3P (Figure 2.14) is the improved version of HRP-2. One of the striking improvement of HRP-3P is that all components or it are designed in a way that they are not affected by water or dust.

Figure 2.14 HRP 2 (on the left side) and HRP-3P (on the right side)

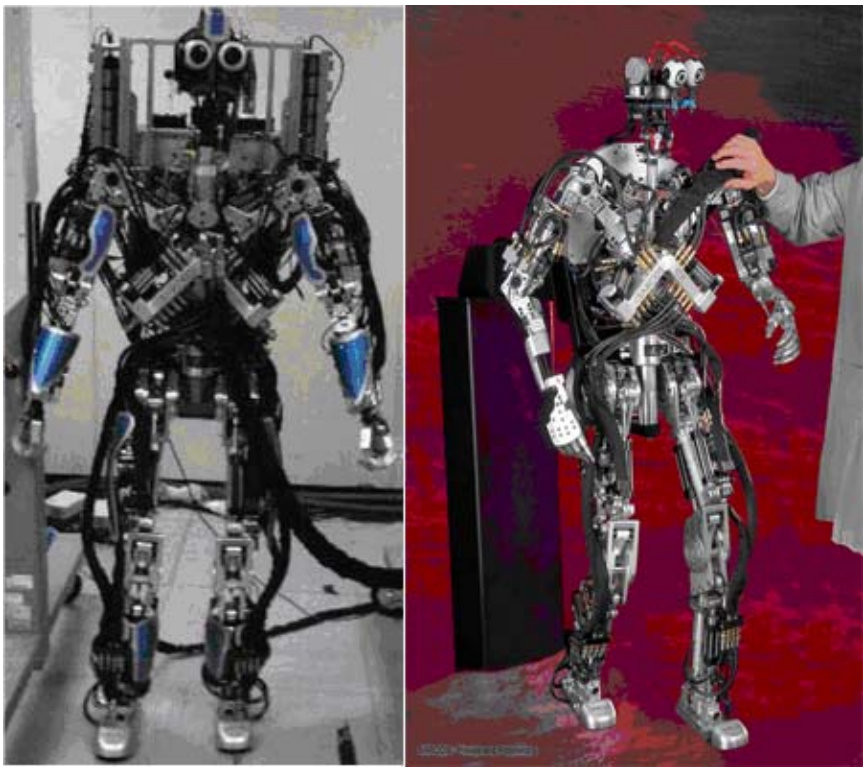

Figure 2.15 DA ATR DB2 Humanoid Robot of SARCOS

Another milestone in humanoid robotics, DA2 ATR DB2 has been developed by SARCOS Company. It is fully hydraulic actuated and no electric motors are used [27, 28] (Figure 2.15).

Walking reference generation and control processes are in progress, but full body balancing, gravity compensation, full body force interaction tasks are achieved. Although its' mechanical design and body parts are not considered to be lightweight, powerful hydraulic actuators compensates this disadvantage and produce a great motion capability which is nearly six times faster that electrically actuated examples. This means that it is nearly capable of doing human actions that need reasonable mobility like jogging, playing ice hockey, juggling or paddling a ball [29]. In addition to this it is capable of online feature recognition by utilizing stereo camera technology.

2.3. Biped Robot Walking Reference Generation

When compared with wheeled or other multi legged robots (quadropedal, six legged, eight legged etc.), it can be easily recognized that bipedal humanoid robot is a better choice for task demands in human living environments. Wheeled robots are considered to serve better on smooth surfaces due to their ground contact geometry. However this geometry does not facilitate obstacle avoidance or rugged terrain consistency. The human environment generally does not consist of smooth ground surfaces. Hence, the mobility of wheeled robots in human environment is limited to smooth and planar surfaces. In addition to this, other multi legged robots can accommodate rugged terrain but may not be suitable for human interaction scenarios such as elderly care, hospital attendance or baby sitting due to their appearance.

Although bipedal walking locomotion is desired due to its harmony to human living environment, bipedal robots have disadvantages like highly non-linear dynamics, high number of degrees of freedom and instability trend too. These complex characteristics make the locomotion hard to execute. Although there are successful examples that can obtain stable bipedal walking these applications still lack in many ways when compared with human walking in stability, robustness, motion capability and flexibility.

Walking reference trajectory generation is of primary significance. A “stable” reference trajectory is desirable because it can simplify the control task.

There are mainly two kinds of approaches in reference generation:

1) Reference generation with full dynamics models.

2) Reference generation with simplified models.

Figure 2.16 P2 of HONDA

First approach utilizes the whole dynamics characteristics of the humanoid robot such as center of mass position of whole body, link inertia matrices and link masses to generate reference walking trajectories. In this approach whole reference generation process is constituted offline and fed to real robot with an online modification. The most remarkable example for this approach is HONDA P2 [30], shown in Figure 2.16.

The P2 algorithm moves the actual ZMP position to an appropriate position by arranging feet's desired positions and orientations. During single support phase, orientation of the supporting foot posture around ZMP is commanded. In double support phase, orientations of both feet posture around ZMP are adjusted.

Another reference generation technique in this category is developed by Kaneko, K. et. al.. The method is implemented by defining constraints on the movements of joints [31]. In this method hip and foot trajectories are generated to determine the rest of the joint reference trajectories to obtain a walking gait. First, constraints of a walking locomotion trajectory are generated. After this step the feet trajectories are generated by 3rd order spline interpolation. Foot motion types are calibrated by setting the values of constraint parameters. Then the hip trajectory is generated by 3rd order spline interpolation with respect to foot motions. With the

assistance of this method stability of walking locomotion is achieved by satisfying the ZMP criterion.

The second type of approaches needs limited information about the dynamics or the biped robot. Some of this information can be listed as cartesian position of center of mass of body, link lengths and link masses. The most effective and the most wide-spread approach which was developed by Kajita, K. and Tani, K. employs the Linear Inverted Pendulum Model (Figure 2.17) [32].

In this approach equations of motion are simplified and decoupled by considering the whole humanoid robot model as a single point-mass. In order to provide simplicity and linearity in dynamics of humanoid walking robot, height of the body (center of mass position) is kept fixed. By keeping the height of the pendulum fixed, equations of motion for the LIPM are decoupled into saggital and coronal planes. Dynamic equations for each plane can be derived by using a 2-D Linear Inverted Pendulum Model for such as x-z and y-z planes. Linear Inverted Pendulum Model is introduced in a two dimensional version by Tani, K. et al [33]. It is extended to the three dimensional version with a similar theoretical method and similar assumptions. As an alternative to the two dimensional Linear Inverted Pendulum Model, Kajita et al introduced the Table Cart model which can help to have a better insight and intuition on LIPM [34, 35]. Figure 2.18 shows the table-cart model.

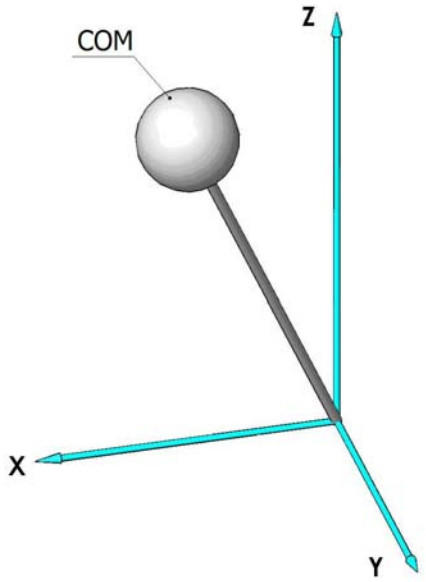

Figure 2.17 Linear Inverted Pendulum Model

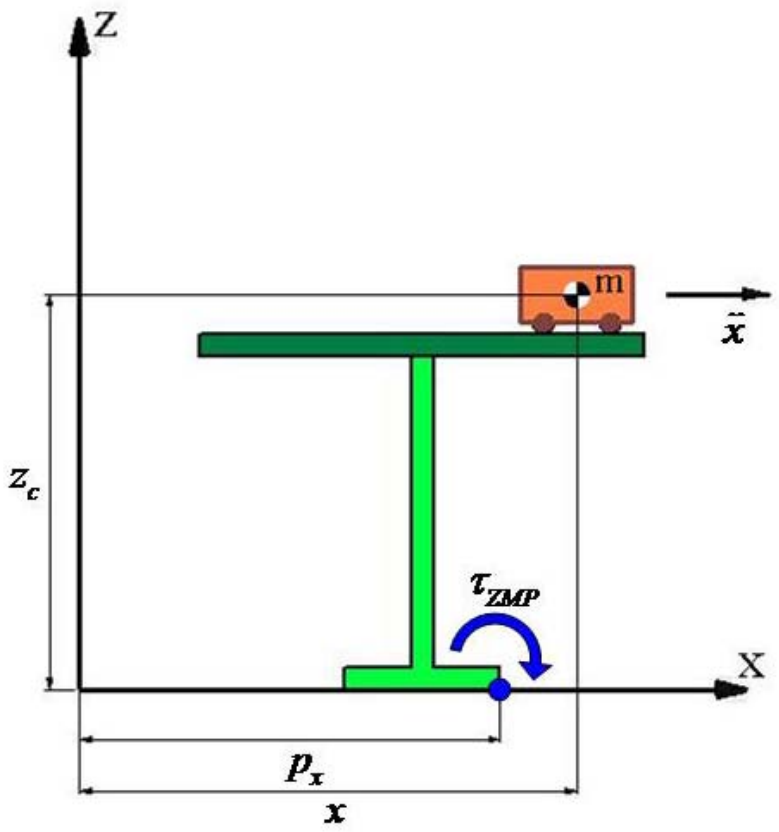

Figure 2.18 Table Cart Model

In order to analyze the dynamics of the table cart model, we should take the gravity effect into consideration. With the torque effect around ZMP which is generated by gravitational force, the cart is expected to fall down and the table is expected to tilt over. In order to prevent such a situation, the cart should have a proper acceleration which will help the table to remain upright for a while. At that moment the ZMP lies inside the supporting polygon. Moment around the ground contact point should be zero. Using the same methodology, equations of motion can be derived for coronal (y-z) plane too. The same set of motion equations is obtained by the LIPM and table-cart models.

This approach is conformable for online computations and feed back control for humanoid robot. Hence it is used by many researchers around the world [36, 37].

After a couple of years, the LIPM is improved by Park and termed as Gravity Compensated Linear Inverted Pendulum Model with the new developments (Figure 2.19) [2].

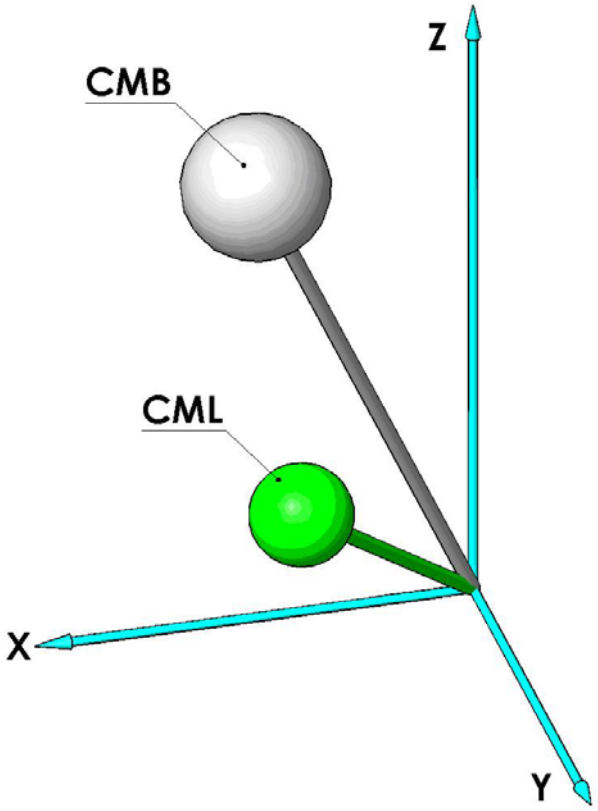

Figure 2.19 Gravity Compensated Linear Inverted Pendulum Model

The addition of new model is related to the swing leg dynamics of the bipedal humanoid robot. In the previous approach that Kajita and Tani introduced, the humanoid robot is considered as a single point-mass and legs are modeled as weightless rods. This assumption, however, does not hold for heavy legs. In order to overcome this problem, Park et al. developed a new Linear Inverted Pendulum Model that includes two point masses. These masses represent the swing leg (Center of Mass of Leg - CML) and the rest of the body (addition of support leg and trunk - CMB) of the humanoid robot. They defined trajectories for the swing leg and the ZMP. Using this strategy, acceleration and resultant moment effects of the swing leg are calculated by taking inertial effects into consideration. These moments and accelerations are included in the model. This model is a similar model to the previous one with some modifications and simplification assumptions.

After those approaches the effects of the Zero Moment Point to the dynamic stability of the humanoid bipedal robot were verified and Zero Moment Point integrated Linear Inverted Pendulum Models are used by researchers around the globe [38, 39, 40].

In all the ZMP and LIPM based reference generation methods, the COM or CMB trajectory for achieving the desired robot ZMP is computed. The joint references are computed then by inverse kinematics. Control algorithms which employ online feedback in order to enhance the walking stability are reported too [41].

Chapter 3

3. THE BIPEDAL HUMANOID ROBOT MODEL

3.1 The Kinematic Arrangement

The humanoid biped robot model used in this thesis is a new conception that is designed and simulated within the context of TÜBİTAK funded project (106E040).

This model is selected as a simulation model due to its realistic design and reasonable link lengths which make the humanoid robot adaptable to human environment. The humanoid robot design consists of two legs with 6 D.O.F. each and a trunk connecting them (Figure 3.1). These conformable link lengths and link masses are shown in Table 3.1.

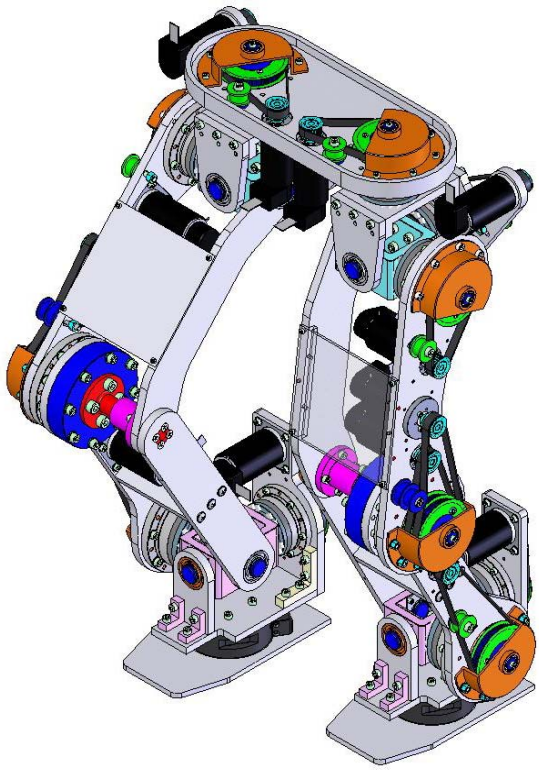

Figure 3.1 Three Dimensional Design of Bipedal Humanoid Robot

Reference coordinate frames are used to represent the relationships between the center of mass of body, foot center and world. These reference coordinate frames are shown in Figure 3.2.

Table 3.1

Link Lengths and Masses

Link	Dimensions (L x W x H) [m]					Mass [kg]
Trunk	0,2	x	0,4	x	0,5	50
Thigh	0,28	x	0,1	x	0,1	7
Calf	0,27	x	0,05	x	0,1	5,5
Foot	0,11	x	0,12	x	0,2	2

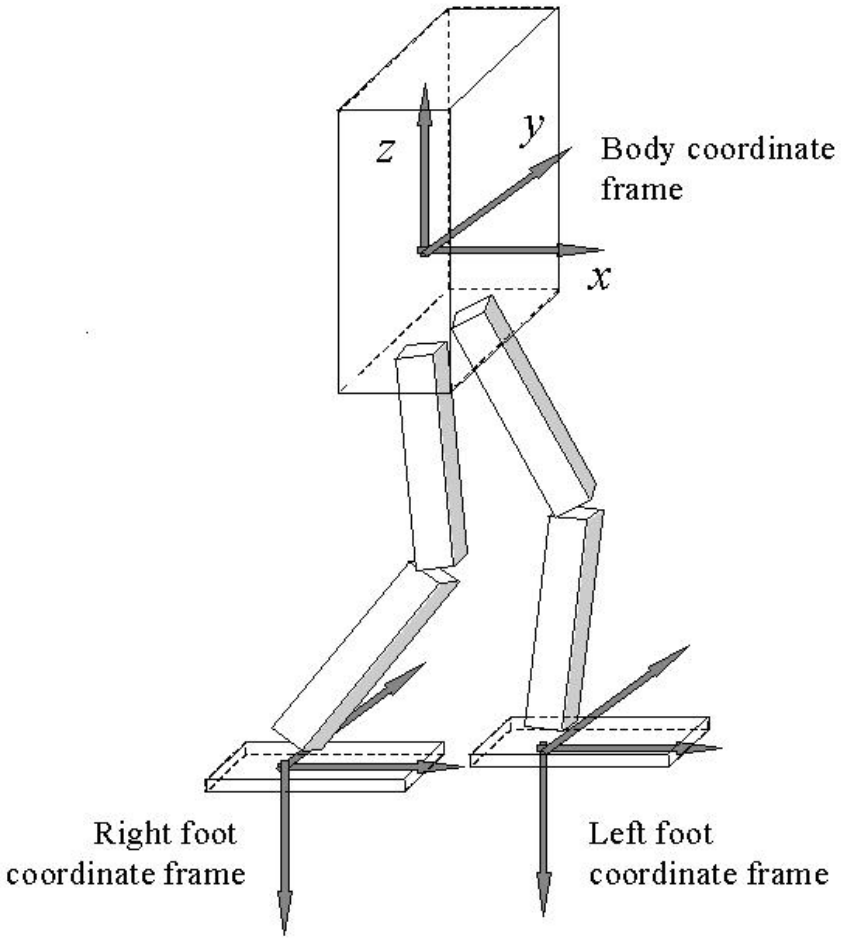

Figure 3.2 The body and the foot coordinate frames.

The Joints and joint axis are assigned according to Denavit-Hartenberg methodology [43]. Joints are shown in Figure 3.3 for the whole model and Joint axis representation is shown in Figure 3.4 for one leg.

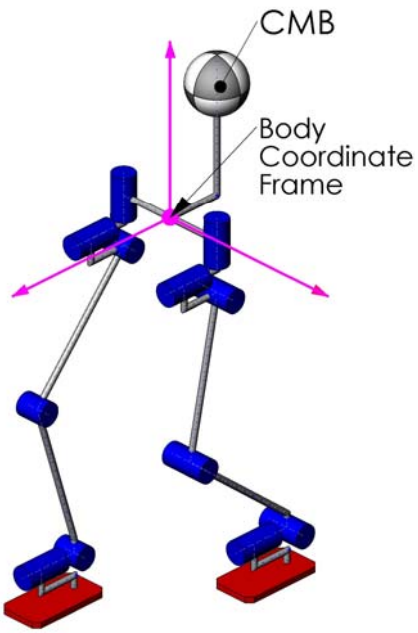

Figure 3.3 Kinematic Arrangement of the biped robot.

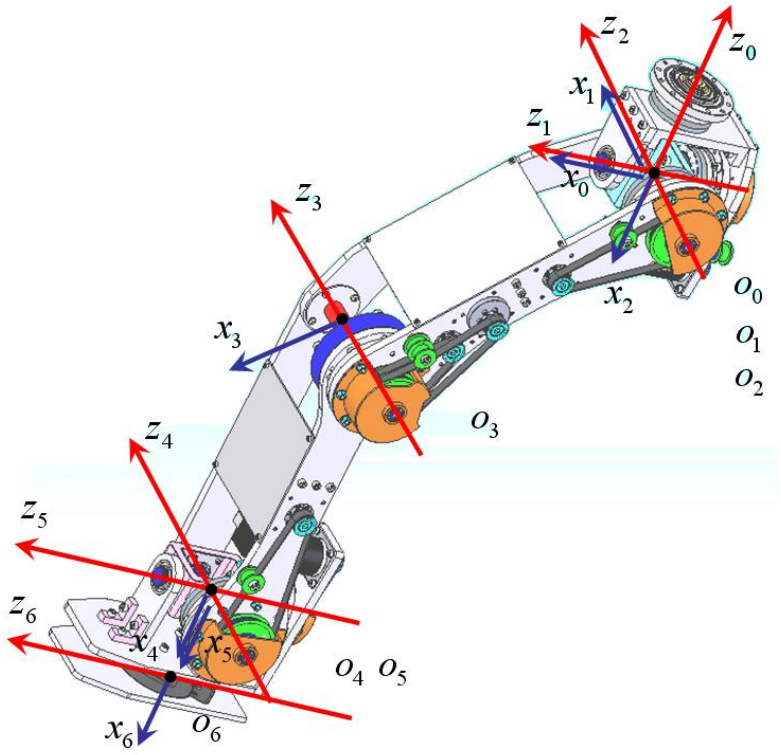

Figure 3.4 Denavit-Hartenberg Joint Axis Representations for One Leg

Table 3.2

Denavit-Hartenberg Parameters of the biped leg

Link	a_i	α_i	d_i	θ_i
1	0	$\pi/2$	0	θ_1^*
2	0	$-\pi/2$	0	θ_2^*
3	L_3	$\pi/2$	0	θ_3^*
4	L_4	0	0	θ_4^*
5	0	$-\pi/2$	0	θ_5^*
6	L_6	0	0	θ_6^*

3.2 Dynamics Equations and Simulation Model

The bipedal humanoid robot is considered to have interaction with the ground but not bonded such as a falling manipulator. The full dynamics description for a robot structure like the one shown in Figure 3.5 is highly nonlinear, multiple dof and coupled. Its motion equation can be expressed as

$$\begin{bmatrix} H_{11} & H_{12} & H_{13} \\ H_{21} & H_{22} & H_{23} \\ H_{31} & H_{32} & H_{33} \end{bmatrix} \begin{pmatrix} \dot{v}_B \\ \dot{\omega}_B \\ \ddot{\theta} \end{pmatrix} + \begin{pmatrix} c_1 \\ c_2 \\ c_3 \end{pmatrix} + \begin{pmatrix} u_{E_1} \\ u_{E_2} \\ u_{E_3} \end{pmatrix} = \begin{pmatrix} 0 \\ 0 \\ \tau \end{pmatrix} \tag{3.1}$$

where H_{ij} for $(i, j) \in \{1,2,3\}$ are sub-matrices of the robot inertia matrix. v_B is the linear velocity of the robot body coordinate frame center with respect to a fixed world coordinate frame, ω_B is the angular velocity of the robot body coordinate frame with respect to a fixed world coordinate frame, and θ is the vector of joint displacements of the biped. The vector formed by augmenting c_1, c_2, and c_3 is termed as the bias vector in this dynamics equation. u_{E_1} is the net force effect and u_{E_2} is the net torque effect of the reaction forces on the robot body. u_{E_3} stands for the effect of reaction forces on the robot joints. Reactive forces are generated by environmental interaction. τ is the generalized joint control vector, typically consisting of joint actuation torques for a robot with revolute joints. H_{11}, H_{12}, H_{21}, and H_{22} are 3×3 matrices. For a 12 dof robot with 6 dof at each leg, as described in the previous section; H_{13} is 3×12, H_{23} is 3×12, H_{31} is 12×3, H_{32} is 12×3, and H_{33} is 12×12 [44]. The closed form solutions of the matrices in this expression are very difficult to obtain. Rather, Newton-Euler recursive formulations are used in their computation [45-46].

A view of the animation window is shown in Figure 3.5. The full-dynamics 3-D simulation scheme is similar to the one in [45]. The ground contact is modeled by an adaptive penalty based method. The details of the simulation algorithm and contact modeling can be found in [46]. This model used in the simulation studies presented in Section V.

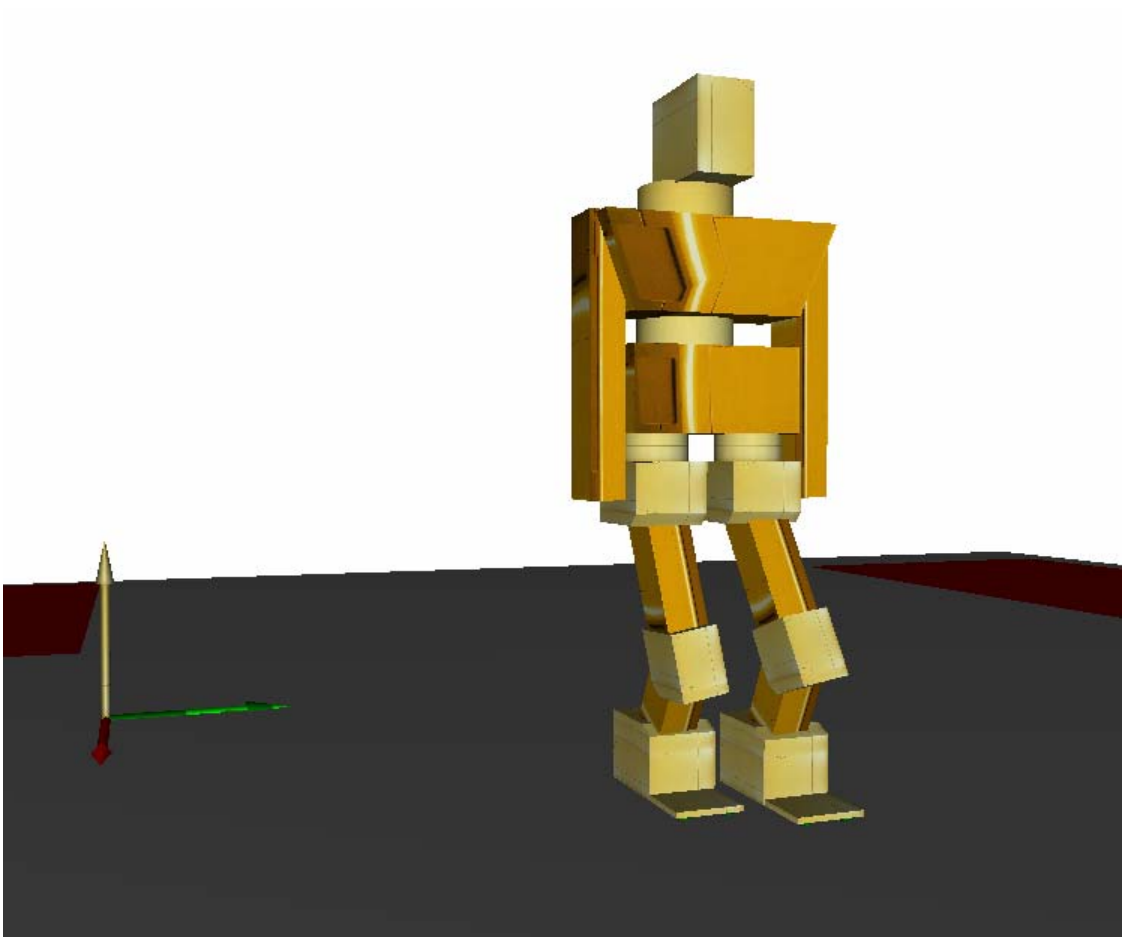

Figure. 3.5 A snapshot from the animation window.

3.3 Inverse Kinematics

In this section inverse kinematics equations for the leg design presented in the previous sections are obtained. This solution is used in the reference generation algorithms presented in the next chapter and in the control method in Chapter 5. The inverse kinematics problem is solved for the six DOF manipulator (leg) between the hip and foot coordinate frames. Without restriction of generality, the solution is obtained for the left leg. The expressions for the right leg are identical since the Denavit-Hartenberg parameter tables of the right and left legs are identical too.

A quite often used way applied for the inverse kinematics of biped walking robots is to employ the Newton-Raphson method. However a closed form solution is more favorable for computational efficiency, both in simulations and for the planned future implementations.

It is well-known that, a closed form solution can be found for industrial type manipulators with a spherical wrist by decoupling the problem into the position inverse kinematics and orientation inverse kinematics problems [42]. A spherical wrist is defined as the combination of three revolute joints which are positioned as the last three degrees of freedom in the kinematic arrangement, with their joint axes intersecting at a common point. Since the ankle of the robot accommodates only two revolute joints, the spherical wrist based decoupling idea can not be implemented as it is done for industrial manipulators. However, the hip structure consists of three revolute joints, and the decoupling of inverse kinematics problems is possible by considering it as a “spherical hip”.

The formal statement of the problem is that the homogeneous transformation matrix $T_{L_0}^{L_6}$ is given and q_L, the joint variable vector for the left leg is wanted. In order to use the spherical hip idea, in the solution procedure, the leg is considered firstly as an upside down manipulator with its base at the robot foot and its tool tip at the hip center shown in Figure 3.4.

The given $T_{L_0}^{L_6}$ is inverted to obtain the desired homogeneous transformation matrix for the foot based manipulator:

$$T_{desired} = \left(T_{L_0}^{L_6}\right)^{-1} \tag{3.2}$$

$T_{desired}$ can be written as

$$T_{desired} = \begin{bmatrix} A_{desired} & d_{desired} \\ 0\,0\,0 & 1 \end{bmatrix} \tag{3.3}$$

If we shift the foot frame in Figure 3.4 up to the ankle without rotating it and add the "ankle length" a_6 to the x_6 direction component we obtain a simpler problem.

This new frame is denoted as (o'_6, x'_6, y'_6, z'_6) and the new desired homogeneous transformation matrix relating the ankle and hip frames is written as

$$T_{desired,ankle} = \begin{bmatrix} A_{desired} & d_{desired} + a_6 \\ 0\,0\,0 & 1 \end{bmatrix} \tag{3.4}$$

Defining $d_{desired,ankle}$ as $d_{desired,ankle} = d_{desired} + a_6$ we can state that the distance between hip and ankle centers is $d_{desired,ankle}$. The basic robot leg model in Figure 3.6 is used in the discussions which follow.

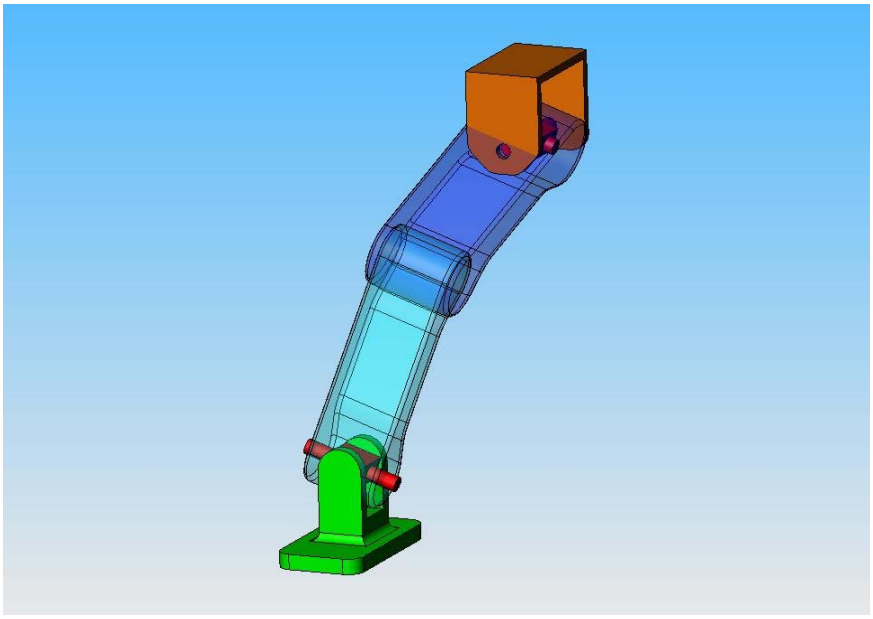

Figure. 3.6 A simple leg structure with the kinematic arrangement described in Table 3.2.

The shank, the thigh and the vector $d_{desired,ankle}$ form a triangle as shown is Figure 3.7. Applying the cosine law on this triangle q_{L4} can be obtained. As

$$\cos(q_{L4}) = \frac{a_3^2 + a_4^2 - \left|d_{desired,ankle}\right|}{2a_3^2 a_4^2} \tag{3.5}$$

Where $\left|\cdot\right|$ stands for vector norm. This yields two solutions for q_{L4}:

$$q_{L4} = a\tan 2(\pm\sqrt{1-\cos(q_{L4})}, \cos(q_{L4})) \tag{3.6}$$

The negative solution corresponds to the "knee front" configuration and it is the one preferred because it is the natural human knee.

Figures 3.8 and 3.9 show the joint variable q_{L_5}. q_{L_5} is defined as the angle between the coronal plane and the shank in Figure 3.8. However, this angle does not change if we see it from a direction normal to the ankle-knee-hip triangle as seen in Figure 3.9. With the indicated lengths and defined of angles in Figure 3.10, q_{L_5} is computed as

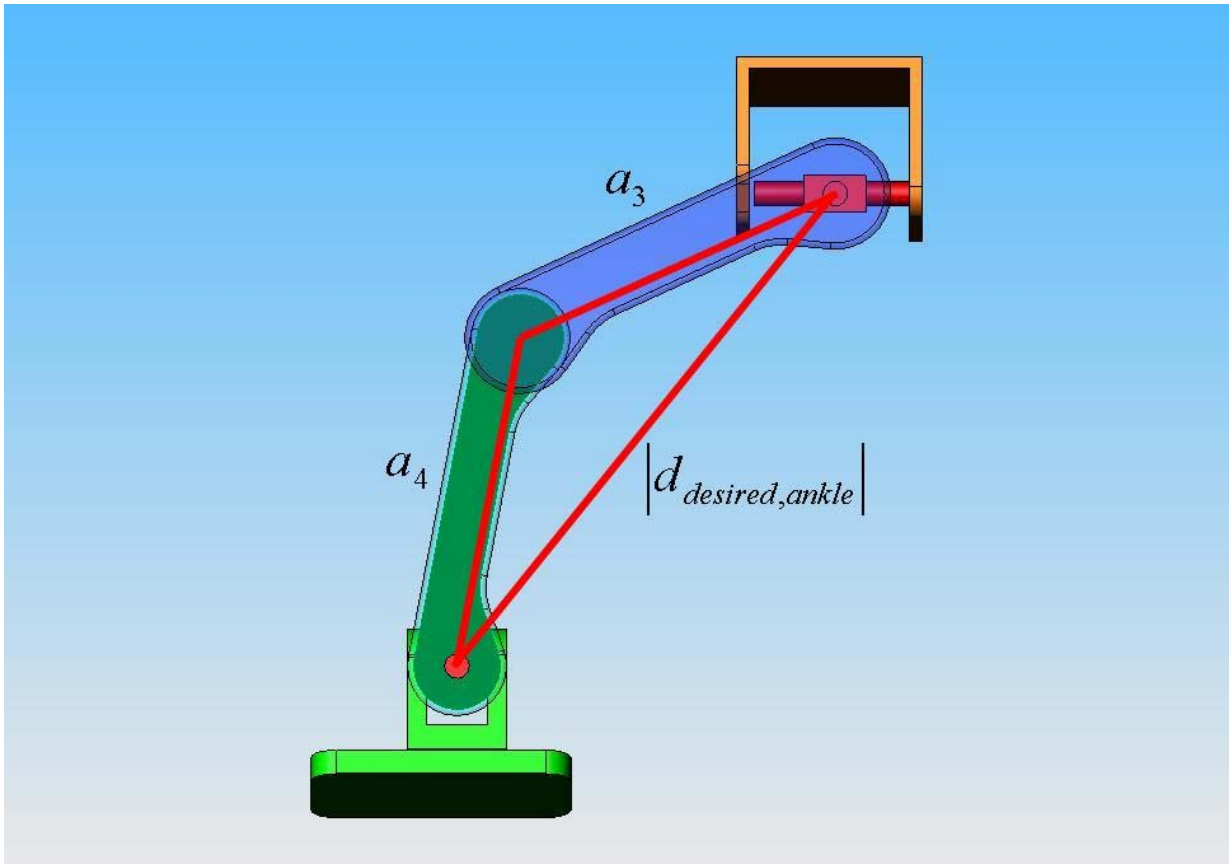

Figure. 3.7 The view normal to the shank and thigh

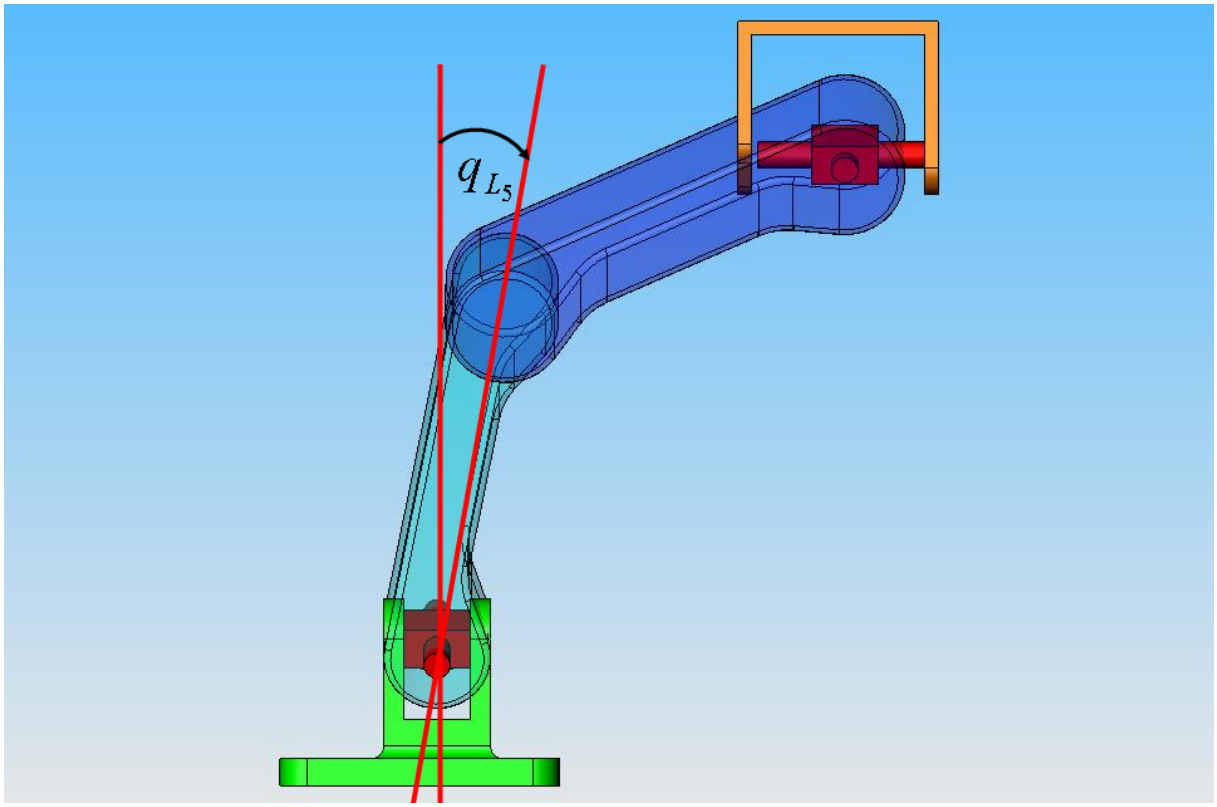

Figure. 3.8 The view normal to the side of the foot

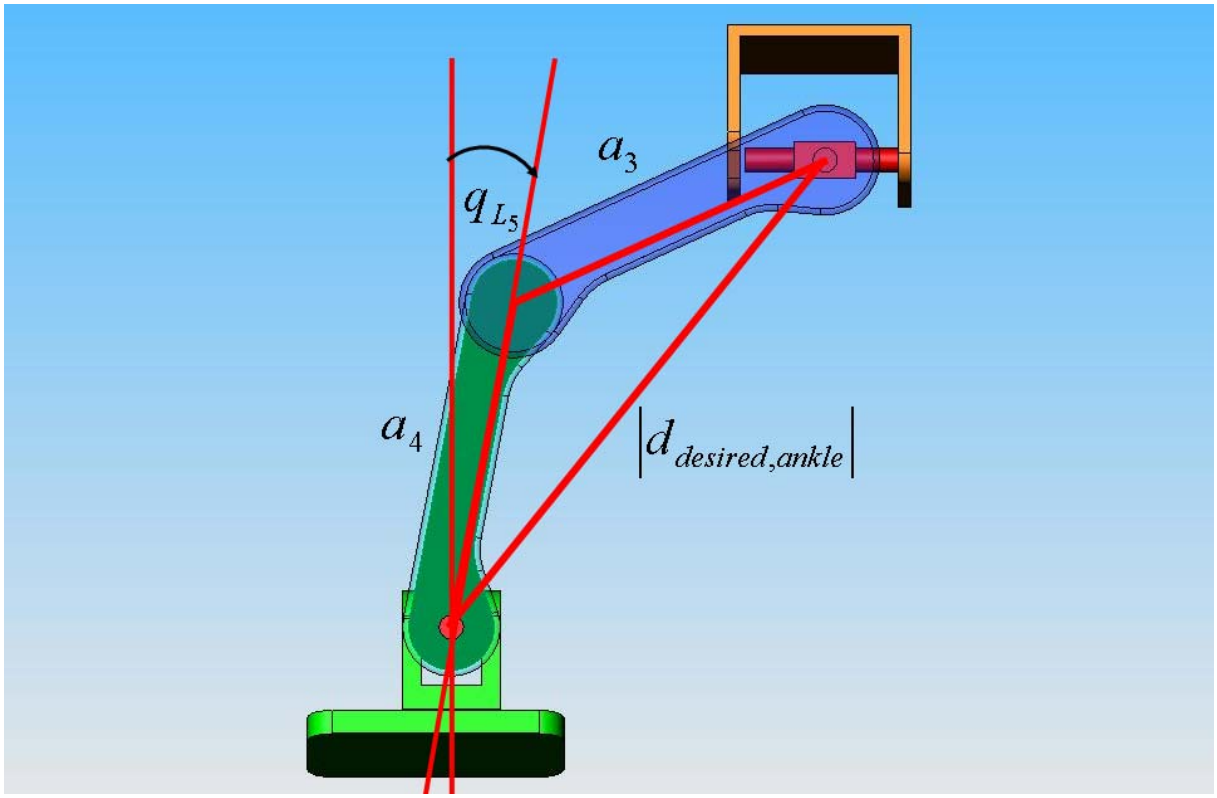

Figure. 3.9 The view normal to the shank and thigh. q_{L_5} is defined in this plane too.

$$q_{L5} = \frac{\pi}{2} - \alpha - \beta \tag{3.7}$$

where

$$\alpha = \text{acos}(-d_{desired,ankle_z} / \left| d_{desired,ankle} \right|) \tag{3.8}$$

and

$$\beta = \text{asin}(a_3 \sin(-q_{L_4}) / \left| d_{desired,ankle} \right|) . \tag{3.9}$$

Finally, q_{L_6} is obtained from Figure 3.11 as

$$q_{L6} = -\text{atan2}(d_{desired,ankle_y}, d_{desired,ankle_x}) . \tag{3.10}$$

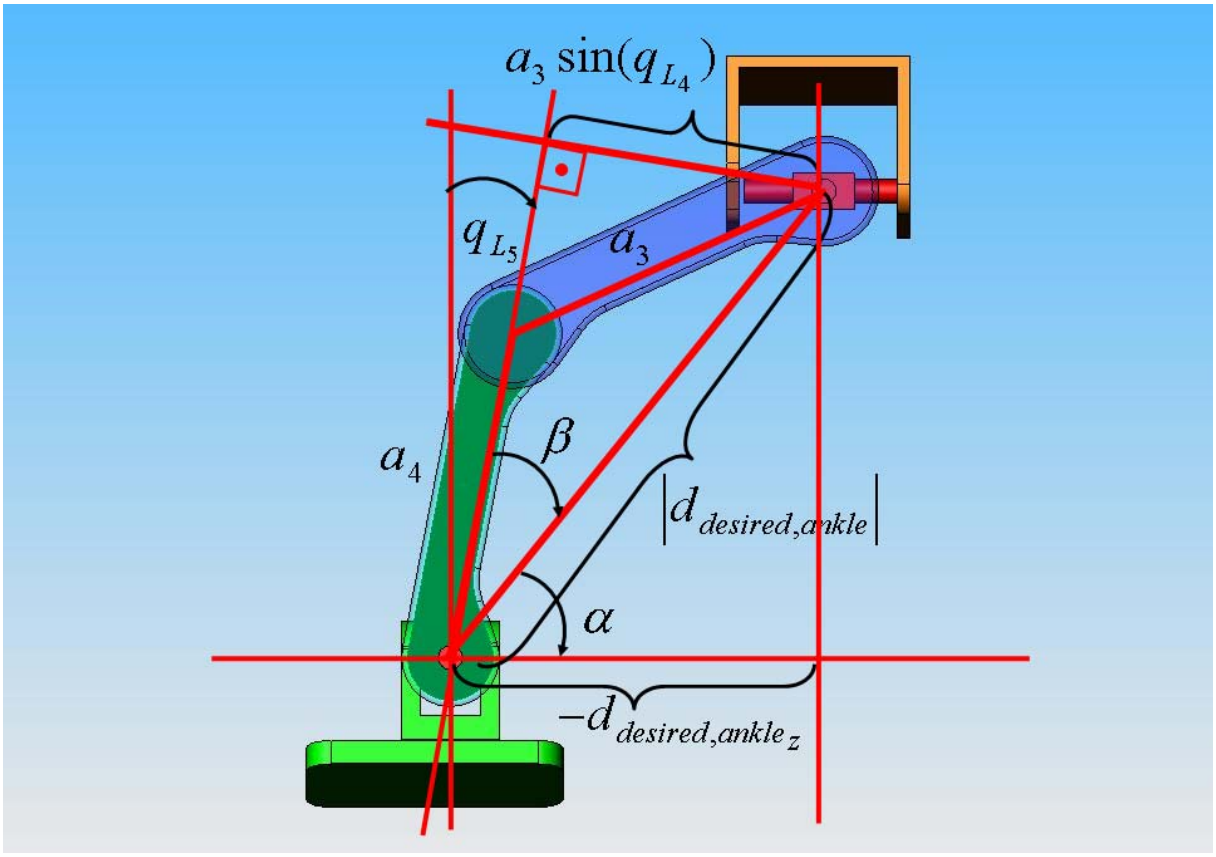

Figure. 3.10 The view normal to the shank and thigh. Computation of q_{L_5}.

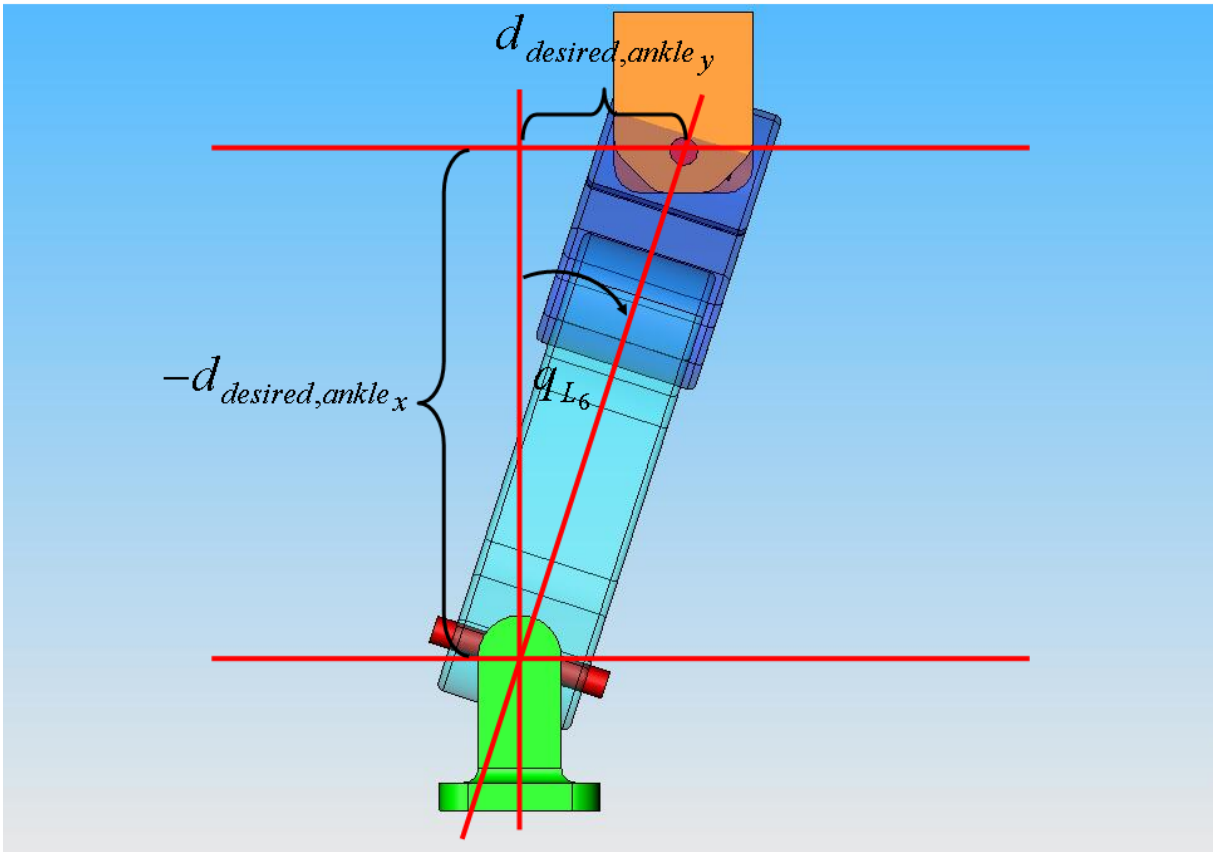

Figure. 3.11 The view normal to the foot front side

In order to obtain the remaining of the joint variables an inverse orientation problem is solved. For this problem, the original given homogeneous transformation matrix $T_{L_0}^{L_6}$ can be employed.

$$T_{L_0}^{L_6} = \begin{bmatrix} A_{L_0}^{L_6} & d_{L_0}^{L_6} \\ 0\,0\,0 & 1 \end{bmatrix} \tag{3.11}$$

where $A_{L_0}^{L_6}$ and $d_{L_0}^{L_6}$ are the wanted orientation matrix and position vector, respectively. For $A_{L_0}^{L_6}$, the following equation holds:

$$A_{L_0}^{L_6} = A(q_{L_1})A(q_{L_2})A(q_{L_3})A(q_{L_4})A(q_{L_5})A(q_{L_6})\,. \tag{3.12}$$

Because q_{L_4}, q_{L_5} and q_{L_6} are computed, the last three rotation matrices in the product above can be computed too. Hence, the product $A(q_{L_4})A(q_{L_5})A(q_{L_6})$ is known at this stage of the inverse kinematics solution. For $A(q_{L_1})A(q_{L_2})A(q_{L_3})$ the following equation holds

$$A(q_{L_1})A(q_{L_2})A(q_{L_3}) = A_{L_0}^{L_6}(A(q_{L_4})A(q_{L_5})A(q_{L_6}))^T \equiv A \tag{3.13}$$

and this defines the inverse orientation problem. The joint variables q_{L_1}, q_{L_2} and q_{L_3} are obtained by solving this equation.

The expression $A(q_{L_1})A(q_{L_2})A(q_{L_3})$ can be written in a more detailed way as

$$A(q_{L_1})A(q_{L_2})A(q_{L_3}) = \begin{bmatrix} c_1c_2c_3 - s_1s_3 & -c_1c_2s_3 - s_1c_3 & c_1s_2 \\ s_1c_2c_3 + c_1s_3 & -s_1c_2s_3 + c_1c_3 & s_1s_2 \\ -s_2c_3 & -s_2s_3 & c_2 \end{bmatrix} \tag{3.14}$$

where c_i stands for $\cos(q_{L_i})$ and s_i is $\sin(q_{L_i})$.

From (3.14), the joint variables q_{L_1}, q_{L_2} and q_{L_3} are obtained as

$$q_{L_1} = \text{atan2}(A_{23}, A_{13}), \tag{3.15}$$

$$q_{L_2} = \text{atan2}(\sqrt{1 - A_{33}^2}, A_{33}) \tag{3.16}$$

and

$$q_{L_3} = \text{atan2}(A_{32}, -A_{31}) \tag{3.17}$$

where the matrix A is as defined in (3.13).

This completes the solution of the inverse kinematics problem.

Chapter 4

4. REFERENCE GENERATION WITH SWING LEG COMPENSATION USING LIPM AND STATE SPACE REPRESENTATION

4.1 ZMP and Foot Position References

ZMP and swing foot references are required for the CMB reference generation computations. The Zero Moment Point criterion states that this point should be under in the supporting polygon of a robot for that robot to be stable. ZMP and swing foot reference generation algorithm employed in this thesis is as presented in [47]. Mainly, the procedure can be summarized as follows:

1) Specify the support foot locations (step size B and foot-to-foot distance $2A$) as in Figure 4.1.
2) Specify the distance travelled by the ZMP under the support foot ($2b$) in the single support phase (Figure 4.2).
3) Specify a walking period ($2T$ in Figure 4.2).
4) Generate x-direction ZMP reference p_x^{ref} (walking direction) as a "staircase of ramps" (Figure 4.2) with the following expression

$$p_x^{ref} = \frac{2b}{T}(t - \frac{T}{2}) + (B - 2b)\sum_{k=1}^{\infty} u(t - kT) \tag{4.1}$$

where u is the unit step function.

5) Generate the y-direction ZMP reference p_y^{ref} with the assumption that the foot switching occurs instantaneously. This corresponds to the square wave shaped reference curve in Figure 4.3:

$$p_y^{ref} = Au(t) + 2A\sum_{k=1}^{\infty}(-1)^k u(t - kT) \tag{4.2}$$

6) Smooth the staircase and square wave shapes to introduce a smooth switching between single support phases (that is, a switching with a double support phase). The resulting ZMP references are shown in Figures 4.4 and 4.5 for the simulation studies presented in this thesis. These are obtained from the curves in Figures 4.2 and 4.3 by the smoothing algorithm in [47].

7) y-direction foot reference positions are constant. The foot x-direction position references in Figure 4.4 are chosen as smooth functions based on sinusoidal building blocks. They are determined by the desired support foot locations (Figure 4.1) and the step period $2T$. The swing foot z-direction references are chosen such that the respective foot is above ground level when the foot x-direction reference is moving forward in Figure 4.4.

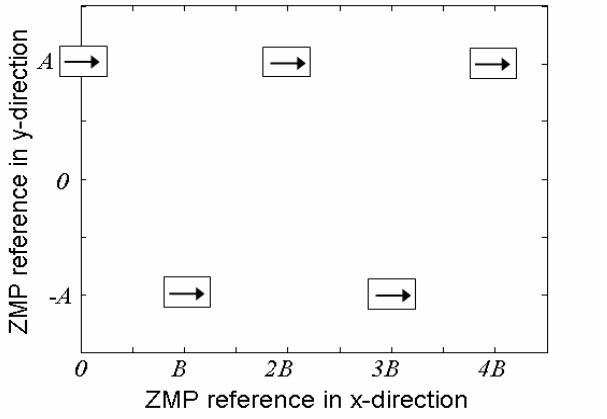

Figure 4.1 Desired foot locations.

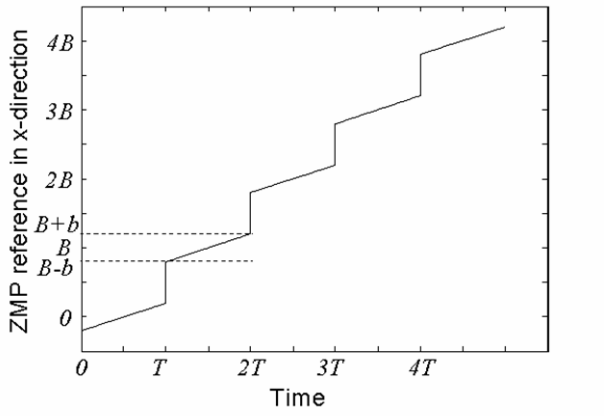

Figure 4.2 ZMP x-direction reference with moving ZMP under the support foot.

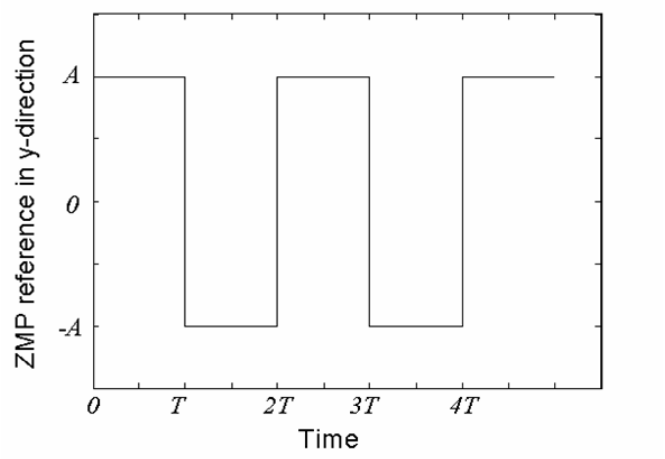

Figure 4.3 ZMP y-direction reference before smoothing.

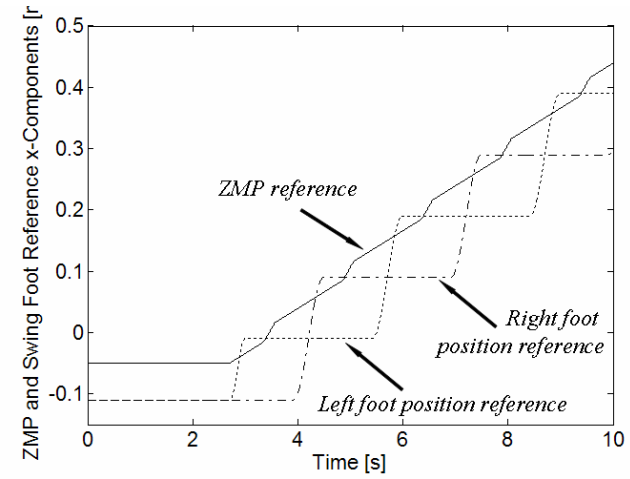

Figure 4.4 ZMP reference after smoothing and swing foot references, x-direction.

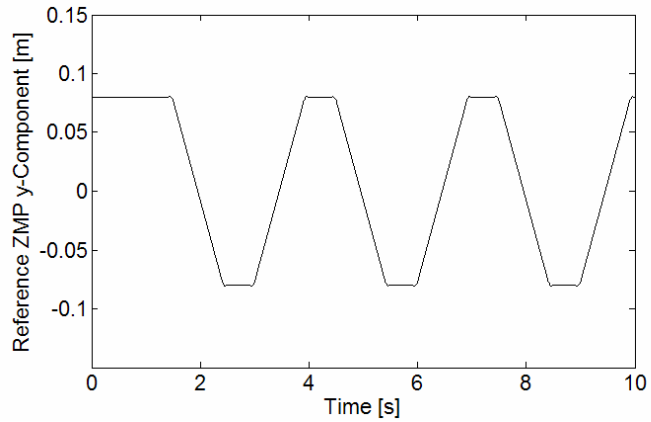

Figure 4.5 ZMP y-direction reference after smoothing.

The orientation references for the body and feet have to be specified too. The body orientation reference with respect to the world coordinate frame is set in such a way that the body is always parallel to the ground. The foot orientation references are aligned with the body frame.

4.2 LIPM Model

Though obtaining a model as in (3.1) is very useful for the simulation and test of reference generation and control methods, this structure is too complex to serve as an intuitive model which can help in developing guidelines and basics for the walking control. Simpler models are more suitable for controller synthesis. The inverted pendulum model is such a simple model. The body (trunk) is approximated by a point mass concentrated at the COM of the robot. This point mass is linked to a stable (not sliding) contact point on the ground via a massless rod, which is the idealized model of a supporting leg. The swing leg is assumed to be massless too. Figure 4.6 shows an inverted pendulum. In this figure, $c = (c_x \quad c_y \quad c_z)^T$ stands for the coordinates of this point mass. Although much simpler than (2.1), the equations of motion of the inverted pendulum model are still coupled and nonlinear. One more assumption, however, yields a linear system which is uncoupled in the x and y-directions. This is the assumption of fixed height of the COM. This model is called LIPM and it is simple enough to work on and devise algorithms for reference generation. The equations of motion of the COM with the LIPM are as follows.

$$\ddot{c}_x = \frac{g}{z_c} x + \frac{1}{mz_c} u_p \tag{4.3}$$

$$\ddot{c}_y = \frac{g}{z_c} y - \frac{1}{mz_c} u_r \tag{4.4}$$

In this equation m is the mass of the body (point mass), z_c is the height of the plane on which the motion of the point mass is constrained, g is the gravity constant (9.806 m/s^2). u_p

and u_r are the pitch (about y-axis) and roll (about x-axis) control torques, respectively. These act at the support point (origin in Figure 4.6) of the linear inverted pendulum.

The idea that the energy efficient references should allow the robot to move in compliance with the natural fall due to the gravity (without too large control effort by the joint actuators) can be employed with this model. References consisting of freely falling (tilting aside) segments are developed in with the LIPM.

Since the solutions of (4.3) and (4.4) in the unactuated case ($u_p = u_r = 0$) are unbounded functions, and therefore, the computation of a reference trajectory from freely falling segments should be carried out carefully in order to obtain a stable reference. Stability of the walk is trivially the most wanted feature of a reference trajectory. In biped robotics, the most widely accepted criterion for stability is based on the location of the ZMP [6]. For the arrangement in Figure 4.6, the zero moment point is defined as the point on the $x-y$ plane about which no horizontal torque components exist. The expressions for the ZMP coordinates p_x and p_y for the point mass structure in Figure 4.6 are in [44] as

$$p_x = c_x - \frac{c_z}{g}\ddot{c}_x \tag{4.5}$$

$$p_y = c_y - \frac{c_z}{g}\ddot{c}_y \tag{4.6}$$

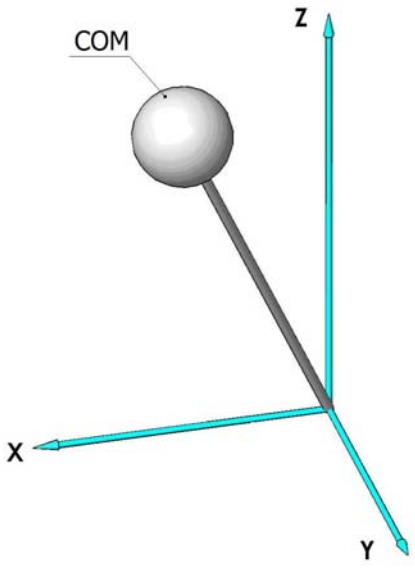

Figure 4.6 Linear Inverted Pendulum Model

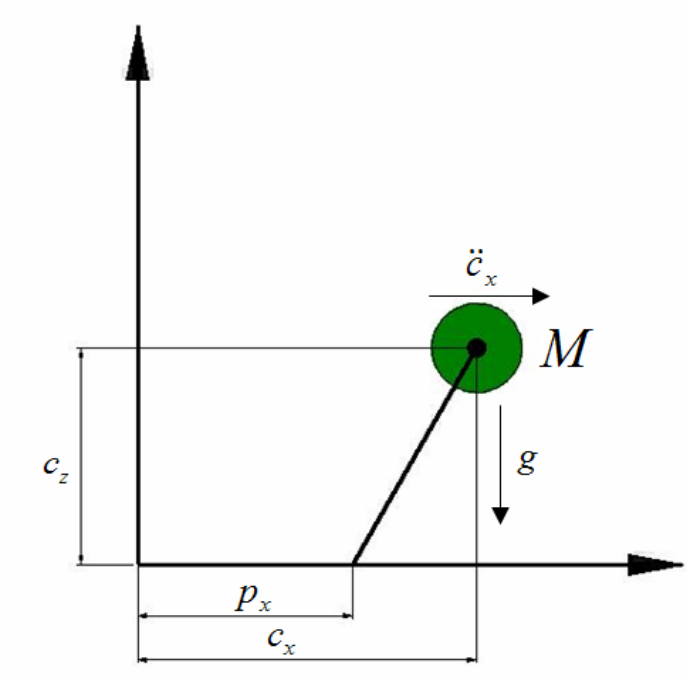

Figure 4.7 One-mass LIPM used in this thesis

The result in (4.5) can be obtained by a torque balance equation in the $x-z$ plane as shown in Figure 4.7.

In order to have zero net moment at the "pivot point" in Figure 4.7, the torque due to gravity (Δxmg) should be balanced by the torque generated by the reaction force due to the acceleration of the point mass in the x direction ($z_c m\ddot{x}$). This gives a solution for Δx and hence, the touching point p_x for the zero moment condition. A similar discussion for the $y-z$ plane can yield (4.6).

Note that when this model serves as a simplified walking robot dynamics description, M stands for the combined mass of the trunk and the legs and c is the location of the overall center of mass, usually abbreviated as COM. However, using the CMB instead of the real COM is also common because of practical reasons.

4.3 State Space Representation and Reference Generation

In this section, a modified version of the ZMP equation (4.5) is introduced. CMB reference generation based on a state space model is discussed. The generalization to the two-mass case will follow. The final reference generation algorithm obtained which uses a combination of the one-mass and two-mass LIPM state space models is discussed lastly.

With (4.5), by applying the Laplace transform we obtain

$$P_x(s) = L(c_x - \omega^2 \ddot{c}_x) \tag{4.7}$$

Where ω is defined as $\sqrt{c_z/g}$. This equation can be used to obtain the c_x trajectory from the given desired p_x trajectory. These approaches followed by a number of studies. However [40] points out that typical ZMP measurement is a noisy one due to the force sensors in the measurement system and adds a low pass filter into the equation:

$$P_x(s) = \frac{1}{1+s\tau} L(c_x - \omega^2 \ddot{c}_x) \tag{4.8}$$

In this equation τ is the filter time constant. Such a filter is typically used in real applications and (4.8) does indeed reflect a realistic situation. [40] uses this model to obtain the state-space description

$$\frac{d}{dt}\begin{bmatrix} p_x \\ c_x \\ \dot{c}_x \end{bmatrix} = \underbrace{\begin{bmatrix} -1/\tau & 1/\tau & 0 \\ 0 & 0 & 1 \\ 0 & 0 & 0 \end{bmatrix}}_{A}\begin{bmatrix} p_x \\ c_x \\ \dot{c}_x \end{bmatrix} + \underbrace{\begin{bmatrix} -\omega^2/\tau \\ 0 \\ 1 \end{bmatrix}}_{B}\ddot{c}_x \tag{4.9}$$

$$p_x = \underbrace{\begin{bmatrix} 1 & 0 & 0 \end{bmatrix}}_{C}\begin{bmatrix} p_x \\ c_x \\ \dot{c}_x \end{bmatrix} + \underbrace{0}_{D}\ddot{c}_x \tag{4.10}$$

and employs (4.9) in feedback control for online stabilization. In this thesis, however, we use this equation for online trajectory generation as follows:

Firstly the continuous state-space realization (*A, B, C, D*) is discretized into a discrete realization (*F, G, H, J*) for computer implementation. A state feedback gain K is obtained by pole placement techniques for stable closed loop pole locations. This gain is used in the block diagram shown in Figure 4.8 where N_x and N_u are the feedforward gain and state reference gain matrices computed as

$$\begin{bmatrix} N_x \\ N_u \end{bmatrix} = \begin{bmatrix} F & H \\ G & J \end{bmatrix}^{-1} \begin{bmatrix} 0 \\ 1 \end{bmatrix} \tag{4.11}$$

The derivation of (4.10) is given in [48] and also in Appendix 1. r in Figure 4.8 is the ZMP x-direction reference. The trajectories of the state variable c_x is stored and used as the robot body center of mass position reference. Since c_x and foot references (Figure 4.4.) are expressed in the same coordinate frame (world coordinate frame), inverse kinematics can be employed to obtain the corresponding joint variable references. PID independent joint controllers are then applied for locomotion control purpose. The robot can indeed walk with this kind of reference trajectory as simulation results in Section V indicate too.

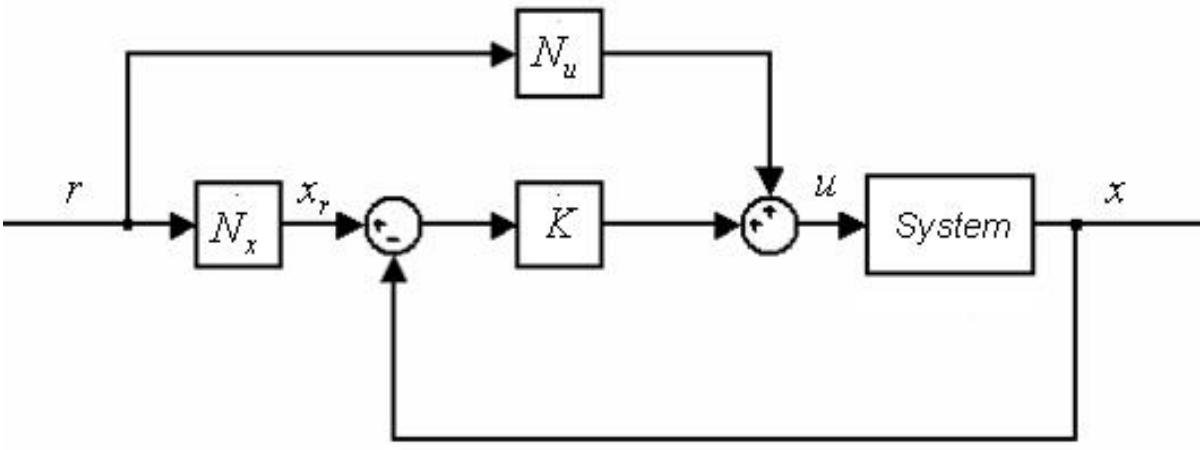

Figure 4.8 State-space description of the system

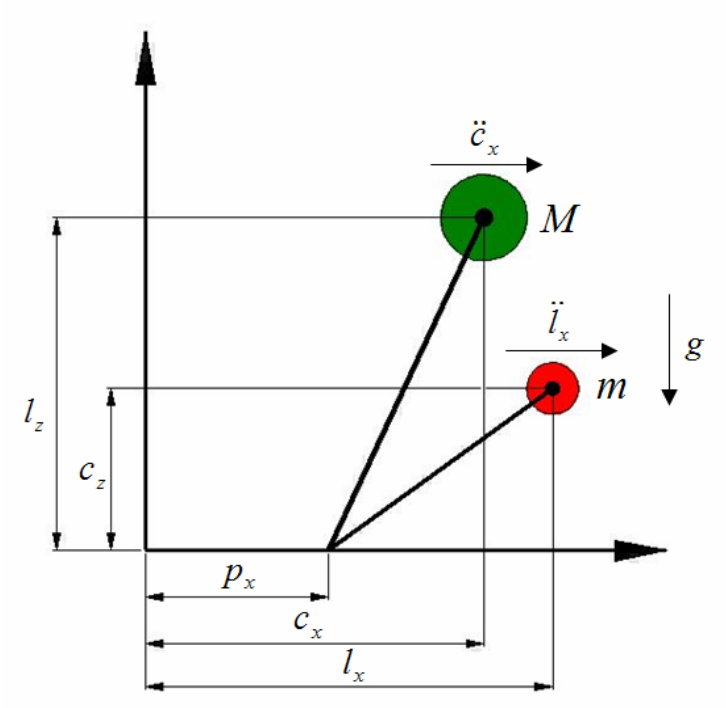

Figure 4.9 A snapshot from the animation window.

However there is a drawback in the single support phases. The weight of the swing leg is not considered in one-mass LIPM and it disturbs the motion of the center of mass during walking. This effect can be identified from front and back, right and left deviations from the planned COM trajectory. In this thesis (as also in [2]), a two-mass LIPM is proposed to alleviate this problem in reference trajectory generation. For the two-mass LIPM, the x-y-plane configuration is shown in Figure 4.9. In this figure defined are two center of mass locations which actually differ from, COM, the overall center of mass of robot.

the robot. c_x now stands for the robot body (or trunk) center of mass, CMB and l_x is the swing leg center of mass, CML. m is the mass of the swing leg. The ZMP equation obtained from Figure 4.9 is as,

$$p_x = \frac{M}{(M+m)} c_x - \frac{M}{(M+m)} \ddot{c}_x \frac{c_z}{g} + \frac{m}{(M+m)} l_x - \frac{m}{(M+m)} \ddot{l}_x \frac{l_z}{g} \tag{4.12}$$

where l_x is the x-directional position of center of mass of swing leg, $\ddot{l}_x$ is the x-directional acceleration of center of mass of swing leg and l_z is the z-directional position of center of mass of swing leg. (4.11) can be put into the form

$$P_x(s) = L(Rc_x - R\ddot{c}_x\omega^2 + rl_x - r\ddot{l}_x\gamma^2) \tag{4.13}$$

where

$$\frac{M}{(M+m)} = R\,, \tag{4.14}$$

$$\frac{m}{(M+m)} = r\,, \tag{4.15}$$

$$\frac{c_z}{g} = \omega^2\,, \tag{4.16}$$

$$\frac{l_z}{g} = \gamma^2 \tag{4.17}$$

The definitions of ω and τ are as for (4.8). Similar to the case with equation (4.8), a low pass filter is added to this equation to obtain

$$P_x(s) = \frac{1}{1+s\tau}(Rc_x - R\ddot{c}_x\omega^2 + rl_x - r\ddot{l}_x\gamma^2) \tag{4.18}$$

With the selection of new state variables as p_x, c_x, $\dot{c}_x$, l_x and $\dot{l}_x$ (4.17) can be realized in state-space as

$$\frac{d}{dt}\begin{bmatrix} p_x \\ c_x \\ \dot{c}_x \\ l_x \\ \dot{l}_x \end{bmatrix} = \underbrace{\begin{bmatrix} -1/\tau & R/\tau & 0 & r/\tau & 0 \\ 0 & 0 & 1 & 0 & 0 \\ 0 & 0 & 0 & 0 & 0 \\ 0 & 0 & 0 & 0 & 1 \\ 0 & 0 & 0 & 0 & 0 \end{bmatrix}}_{F}\begin{bmatrix} p_x \\ c_x \\ \dot{c}_x \\ l_x \\ \dot{l}_x \end{bmatrix} + \underbrace{\begin{bmatrix} -R\omega^2/\tau & -r\gamma^2/\tau \\ 0 & 0 \\ 1 & 0 \\ 0 & 0 \\ 0 & 1 \end{bmatrix}}_{G}\begin{bmatrix} \ddot{c}_x \\ \ddot{l}_x \end{bmatrix} \tag{4.19}$$

By setting the output vector y as $[p_x \quad l_x]^T$, the output equation is obtained as,

$$y = \underbrace{\begin{bmatrix} 1 & 0 & 0 & 0 & 0 \\ 0 & 0 & 0 & 1 & 0 \end{bmatrix}}_{H}\begin{bmatrix} p_x \\ c_x \\ \dot{c}_x \\ l_x \\ \dot{l}_x \end{bmatrix} + \underbrace{\begin{bmatrix} 0 & 0 \\ 0 & 0 \end{bmatrix}}_{J}\begin{bmatrix} \ddot{c}_x \\ \ddot{l}_x \end{bmatrix} \tag{4.20}$$

Again this system discretized into a discrete state space realization (F, G, H, J) and a suitable state feedback gain K is obtained by pole placement. A suitable set for a feed forward gain and state reference gain can be found from (4.10).

The simulation runs again in accordance with the block diagram in Figure 4.9 for the two-mass case. However the reference vector is now accommodating the ZMP x-direction reference and the swing leg center of mass x-direction reference l_x. The leg center of mass locations are computed from the current CMB value and swing foot references at every computation cycle by computing the link center of mass coordinates. The history of c_x is stored to be employed as the robot body center of mass reference in the walking time. Inverse kinematics and PID controllers are also employed as in the one-mass case.

The one-mass and two-mass models are used during the trajectory generation simulation alternatingly: When the robot is in the double support phase, the one-mass model is used and the two-mass model is used in the single support phase. Continuity is addressed by reinitializing the starting conditions every time the model switching occurs.

All the discussions above are for the x-direction. However, for the y direction, the deviations are very similar. The whole approach is also applied for the y-directional case and references are obtained for this direction too. As a result these two results are combined to realize the reference for the CMB.

Chapter 5

5. CONTROL OF LOCOMOTION

In this chapter the control method employed for the tracking of the walking trajectories developed by the method in Chapter 4 is discussed.

The references to be followed are specified as the CMB and foot trajectories as expressed in the world frame. Firstly, the joint angle references are obtained by inverse kinematics from the given references. An independent joint PID controller scheme is used for joint space position control.

This method uses the robot joint positions as feedback. However in the biped walking robot terminology this kind of control is still termed as open loop control, since there is no feedback from the environmental interaction (force or tactile information from foot-ground contact) nor from the position and orientation of the body in the world coordinate frame. This means that no corrective actions are taken by the control algorithm against large body inclination angles, slipping foot, or other indications of lost balance during walking. Still this kind of algorithm is suitable for the purpose of this study. In Chapter 6, simulation results of a one-mass model generated reference trajectory is compared with the results of a two-mass model generated trajectory. Since there is no feedback on the balance status of the robot utilized in the control algorithm; the performance, success or failure of the walk will primarily be determined by the performance of the reference generation method.

As explained in Chapter 4, the desired ZMP and desired foot positions are defined firstly, as the primary references. The CMB desired trajectory is obtained as a secondary reference for realizing ZMP references under the given conditions (positions) of the feet.

The inverse kinematics method in Chapter 3 is used to obtain the joint variables corresponding to the given CMB and foot position references. Figures 5.1 and 5.2 summarize the known (given) position vectors for the inverse kinematics problem.

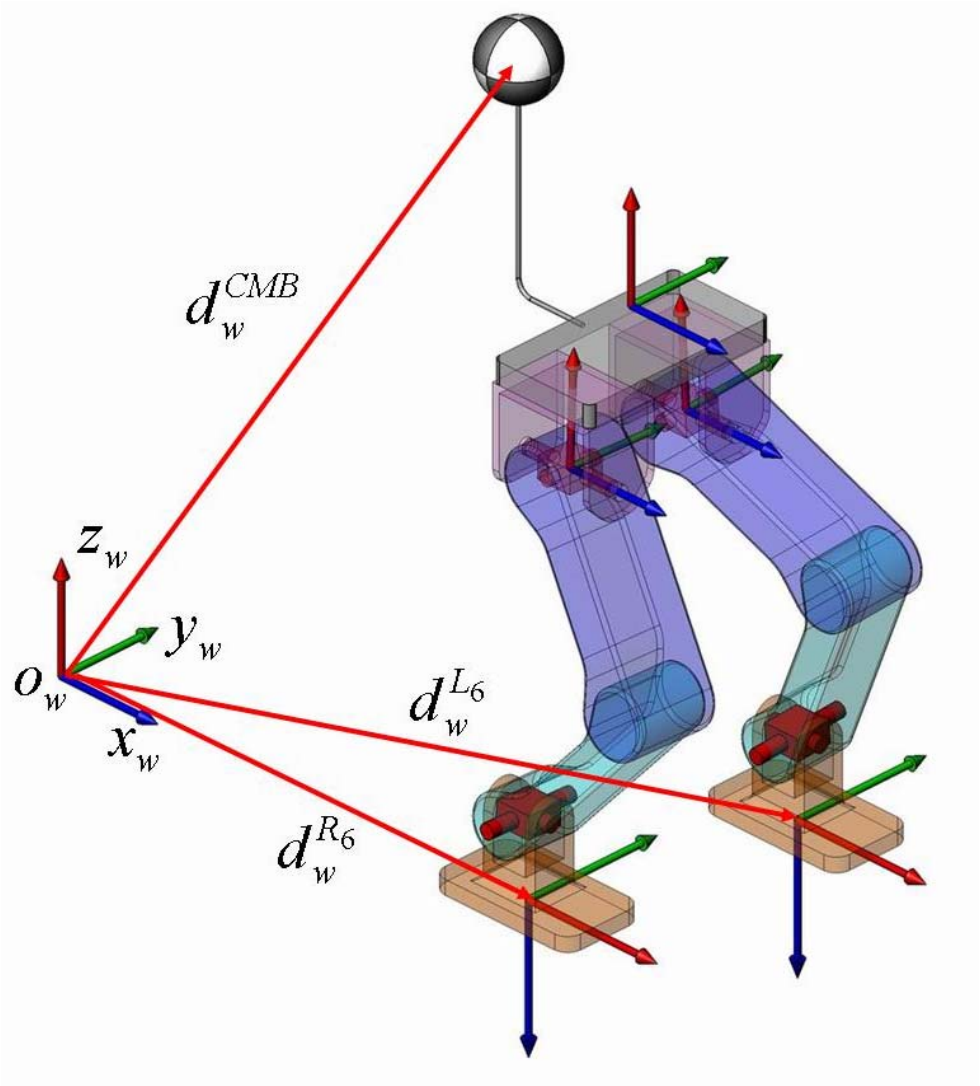

Figure 5.1 Given position vectors defined in the world coordinate frame for the inverse kinematics problem

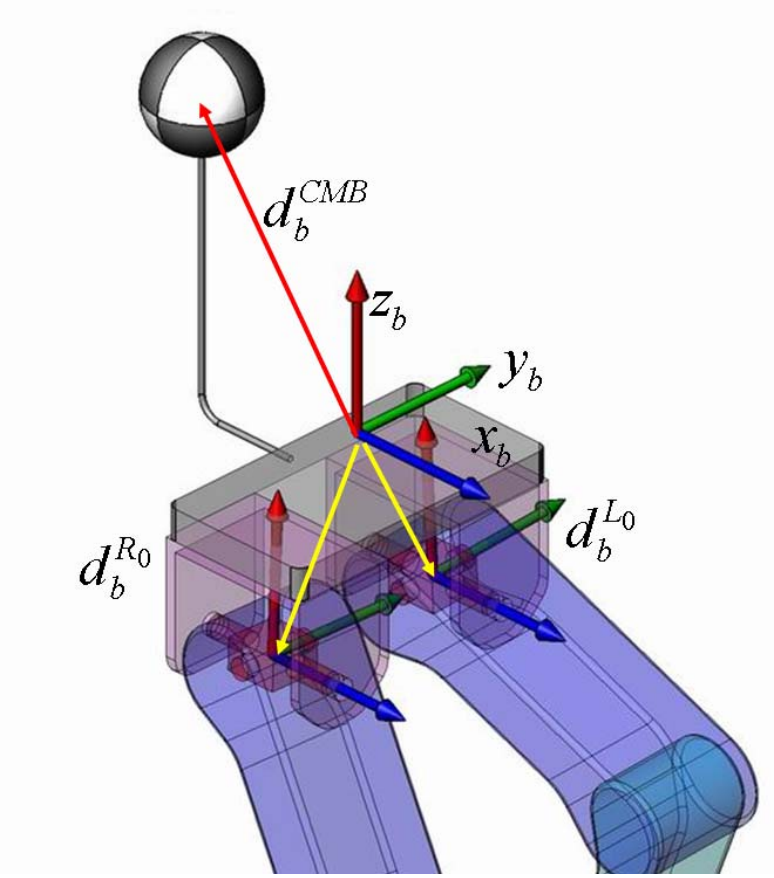

Figure 5.2 Given position vectors defined in the body coordinate frame for the inverse kinematics problem

In addition to the known vectors in these figures, also known is the body frame orientation with respect to the world frame as part of the reference trajectory generation: It is given that these two frames are parallel to each other. Further, according to the reference generation the feet soles should be kept parallel to the body too.

The position vectors shown in Figure 5.3 constitute the position problem definition for the inverse kinematics algorithm in Chapter 3 and in the following they are computed by using the position vectors shown in Figures 5.1 and 5.2.

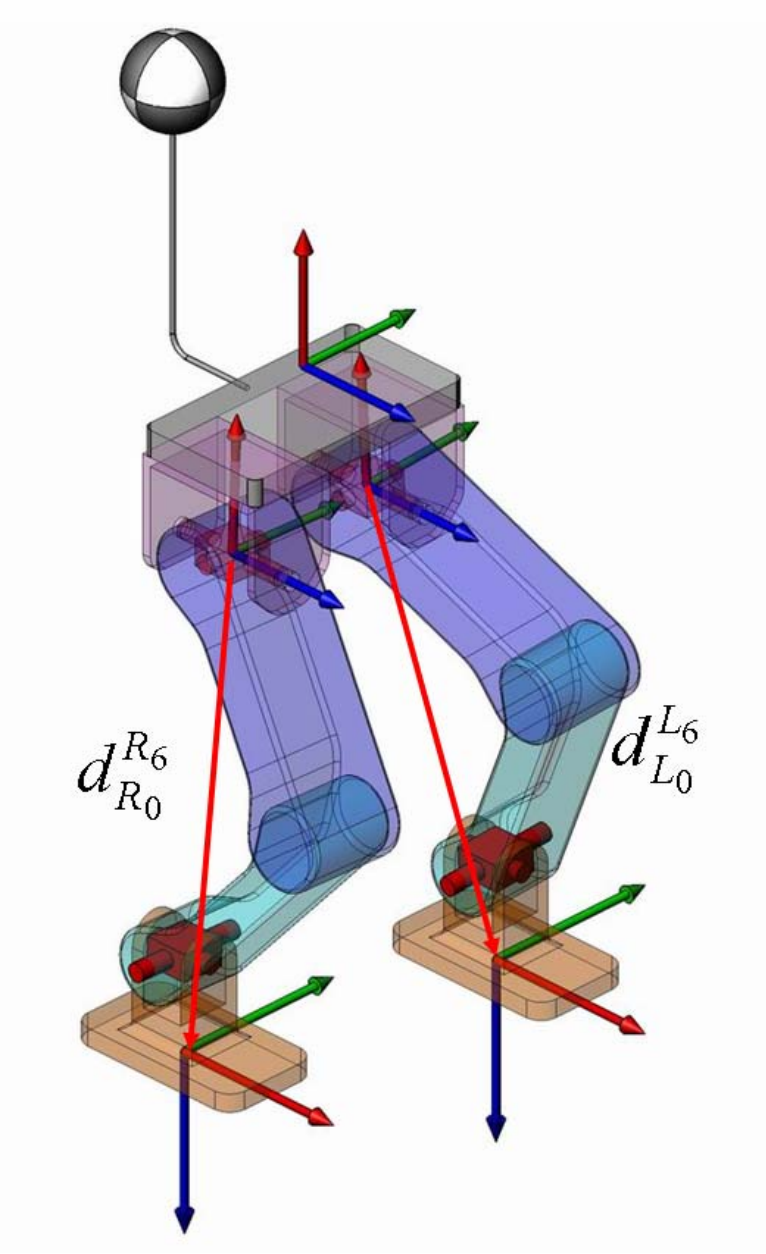

Figure 5.3 The position inputs of the inverse kinematics problem

The computations are presented for the left leg in the following. The equations for the right leg are very similar and therefore not presented here.

Since the inverse kinematics algorithm in Chapter 3 uses the foot position and orientation as expressed in the associated hip frame, the following computations have to carried out to obtain d_{L0}^{L6}, the vector from the left hip frame center to the left foot frame center. The body coordinates in the world frame are

$$d_w^b = d_w^{CMB} - A_w^b d_b^{CMB} \tag{5.1}$$

Because it is given that the body and world frames are parallel, we have

$$A_w^b = \begin{bmatrix} 1 & 0 & 0 \\ 0 & 1 & 0 \\ 0 & 0 & 1 \end{bmatrix} \tag{5.2}$$

and

$$d_w^b = d_w^{CMB} - d_b^{CMB}. \tag{5.3}$$

Next, the left hip position in the world coordinates is found as

$$d_w^{L_0} = d_w^b - A_w^b d_b^{L_0}. \tag{5.4}$$

The vector pointing from the left hip frame center to the left foot, expressed in the world coordinate frame is $d_w^{L_6} - d_b^{L_0}$ and in the left hip coordinated, this vector is expressed as

$$\begin{aligned} d_{L_0}^{L_6} &= A_{L_0}^w (d_w^{L_6} - d_b^{L_0}) \\ &= A_{L_0}^b A_b^w (d_w^{L_6} - d_b^{L_0}) \\ &= A_{L_0}^b (d_w^{L_6} - d_b^{L_0}) \\ &= \left(A_b^{L_0}\right)^T (d_w^{L_6} - d_b^{L_0}) \end{aligned} \tag{5.5}$$

With the axis assignment in Chapter 3,

$$A_b^{L_0} = \begin{bmatrix} 1 & 0 & 0 \\ 0 & 1 & 0 \\ 0 & 0 & 1 \end{bmatrix} \tag{5.6}$$

and therefore we obtain

$$d_{L0}^{L6} = d_w^{L_6} - d_b^{L_0}. \tag{5.7}$$

$d_{L_0}^{L_6}$ is one of the final inputs to the inverse kinematics algorithm, the other one being $A_{L_0}^{L_6}$. With the orientation reference of the body parallel to the ground and feet parallel to the ground the constant foot orientation with respect to the body frame can be computed too. The For Denavit-Hartenberg frames introduced in Chapter 3,

$$A_b^{L_6} = \begin{bmatrix} 0 & 0 & 1 \\ 0 & 1 & 0 \\ -1 & 0 & 0 \end{bmatrix} \tag{5.8}$$

With (5.8)

$$\begin{aligned} A_{L_0}^{L_6} &= A_{L_0}^{b} A_b^{L_6} \\ &= \left(A_b^{L_0}\right)^T A_b^{L_6} \\ &= \begin{bmatrix} 1 & 0 & 0 \\ 0 & 1 & 0 \\ 0 & 0 & 1 \end{bmatrix} A_b^{L_6} \\ &= A_b^{L_6} = \begin{bmatrix} 0 & 0 & 1 \\ 0 & 1 & 0 \\ -1 & 0 & 0 \end{bmatrix}. \end{aligned} \tag{5.9}$$

With $d_{L_0}^{L_6}$ and $A_{L_0}^{L_6}$ we can call the inverse kinematics procedure of Chapter 3 to obtain $q_{L_{ref}}$, the joint variable vector of the left leg. The computations for the right leg can be carried out very similarly, just by replacing the indices L_0 and L_6 by R_0 and R_6, respectively.

A PID controller for the tracking of $q_{L_{ref}}$ is constructed as follows: The position error e_L is defined as

$$e_L = q_{L_{ref}} - q_L, \tag{5.10}$$

where q_L is the vector of actual left leg joint positions. The derivative of the error e_L is approximated by

$$\dot{e}_L(k) = \frac{e_L(k) - e_L(k-1)}{T_s} \tag{5.11}$$

where T_s is the control period, and k is the control cycle index. The integral i_L of the error is computed as

$$i_L(k) = i_L(k-1) + T_s e_L(k). \tag{5.12}$$

Diagonal gain matrices K_p, K_d and K_i are used in the control law for the left leg joint control torque vector τ_L:

$$\tau_L = K_p e_L + K_d \dot{e}_L + K_i i_L \,. \tag{5.13}$$

Suitable values for the entries of K_p, K_d and K_i are obtained by trial and error.

In the next chapter, simulation results are presented with this control algorithm and LIPM based reference generation techniques.

Chapter 6

6. SIMULATION RESULTS

In this section, a walking trajectory with the parameters listed in Table 6.1 is considered. Two cases are simulated:

1) CMB trajectory generated with a one-mass model [49] for double and single support phases with the ZMP and swing foot references in Chapter 4.

2) CMB trajectory generated by the one-mass-two-mass switching model with the ZMP and swing foot references in Chapter 4. The choices for the body and leg mass and heights are given in Table 6.2 The leg and body heights are obtained from typical walking simulations by the trajectory generation in [49] and they are further tuned by trial and error for good walking performance. Figures 6.1-6.3 show the first case (the one-mass case). Deviations from the planned COM trajectory are observed in the swing phases in both x and y directions. The tracking in the double support phase is more successful than in the single support phase. The CMB reference and actual trajectories for the second case (one-mass-two-mass model alternating case) are shown in Figures 6.4-6.6. It can be observed that a swing phase CMB tracking performance is better with the one-mass-two-mass switching reference generation model. This indicates that the effect of the swing foot weight is indeed decreased by the reference generation algorithm. The results for both of the one-mass and one-mass-two-mass switching cases are obtained with the inverse kinematics based open loop position controller without any feedback from the body inclination angles, body position and ground interaction sensors during the walk. Therefore, their performances are purely determined by the performances of the reference generation algorithms. This indicates that the one-mass-two-

mass reference generation algorithm is superior to the one-mass LIPM based reference generation.

Table 6.1
Some of the important simulation parameters

Parameter	**Value**
Step height	0.02m
Step period	3 s
Foot to foot y-direction distance	0.16m
Foot to foot y-direction ZMP reference distance	0.2m
Step size	0.2m
ZMP motion under the support foot	0.08m

Table 6.2
Some of the important simulation parameters

One-Mass Model		**One-Mass-Two-Mass Model**	
Parameter	**Value**	**Parameter**	**Value**
c_z	0.77m	c_z	0.77m
M	86kg	M	68kg
		l_z	0.31m
		m	10kg

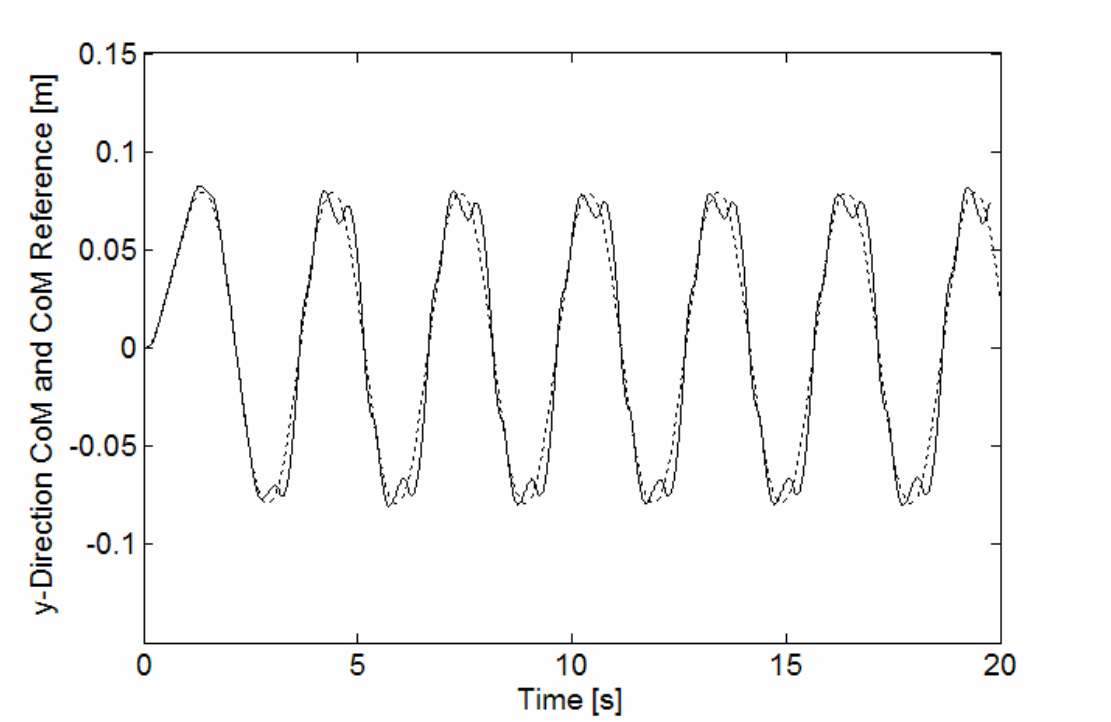

Figure 6.1 CMB position and CMB reference position y-direction curves with the one-mass LIPM. The actual curve is plotted solid. Dotted curve belongs to the reference CMB.

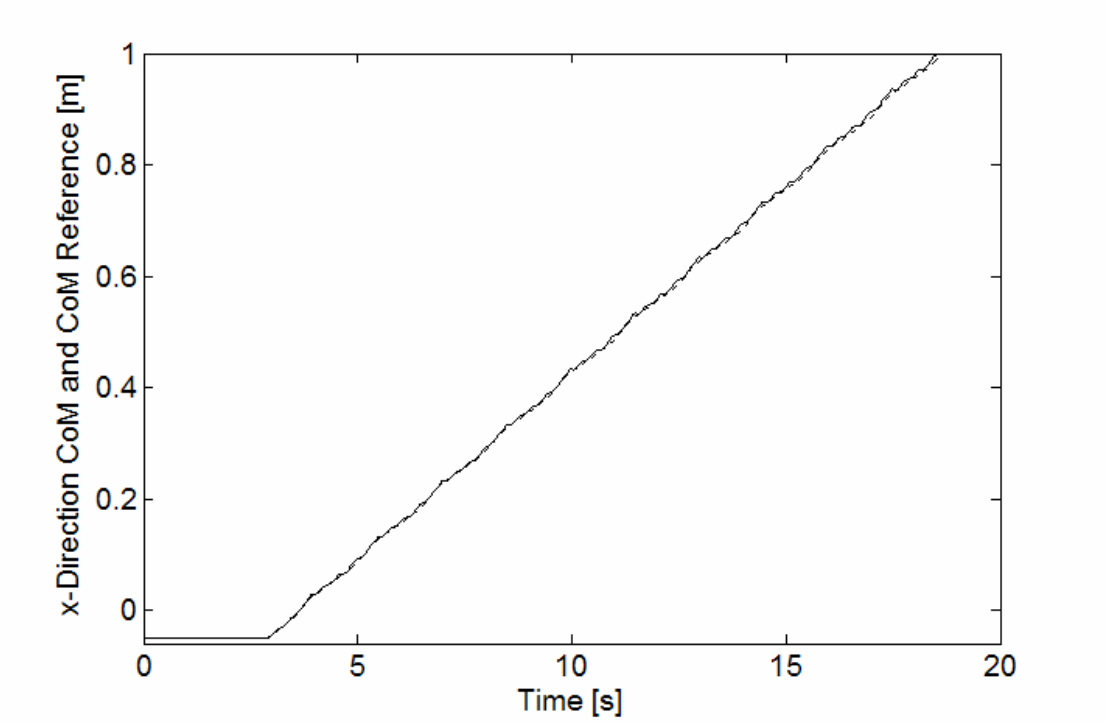

Figure 6.2 CMB position and CMB reference position x-direction curves with the one-mass LIPM. The actual curve is plotted solid. Dotted curve belongs to the reference CMB.

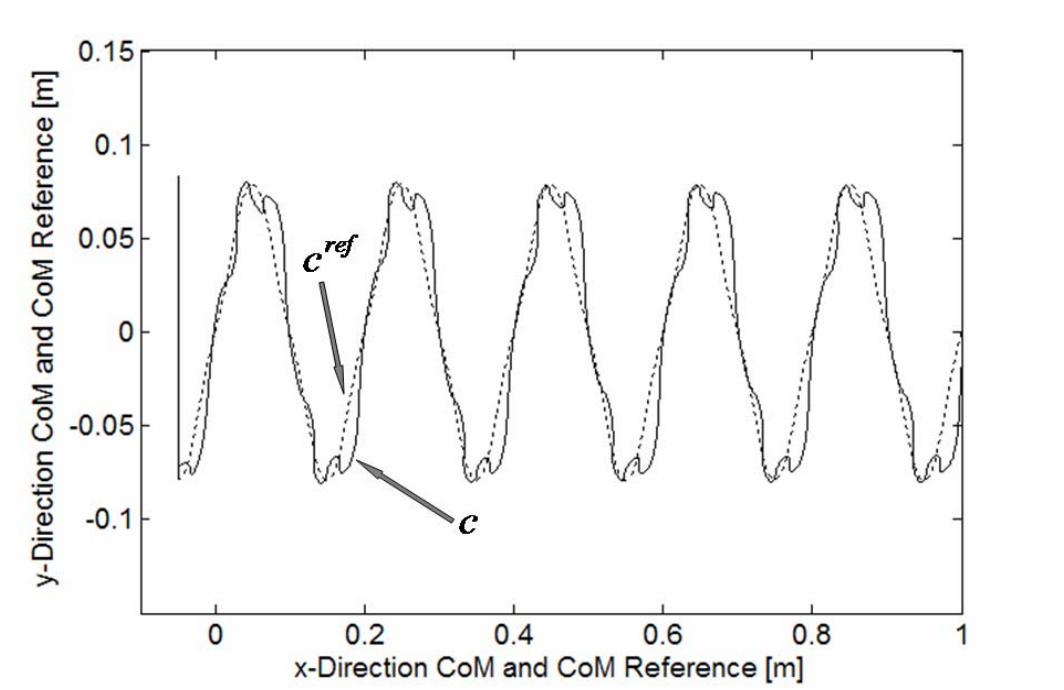

Figure 6.3 CMB position and CMB reference position projections on the *x*-*y*-plane (ground plane) with the one-mass LIPM.

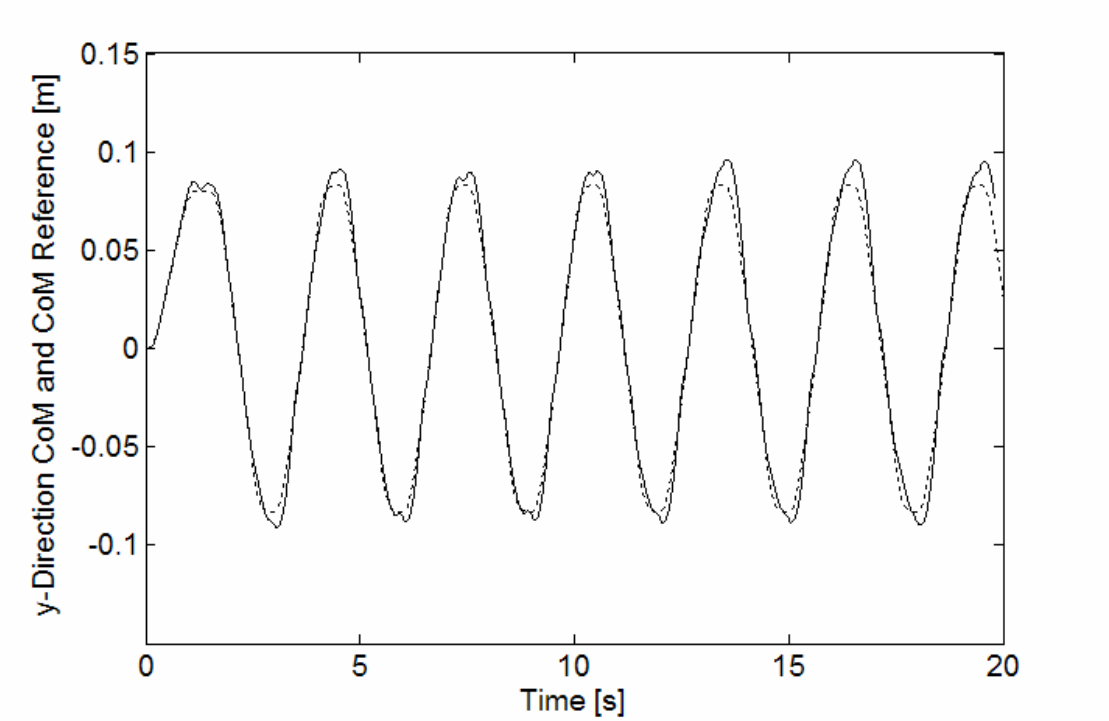

Figure 6.4 CMB position and CMB reference position y-direction curves with the one-mass-two-mass switching LIPM. The actual curve is plotted solid. Dotted curve belongs to the reference CMB.

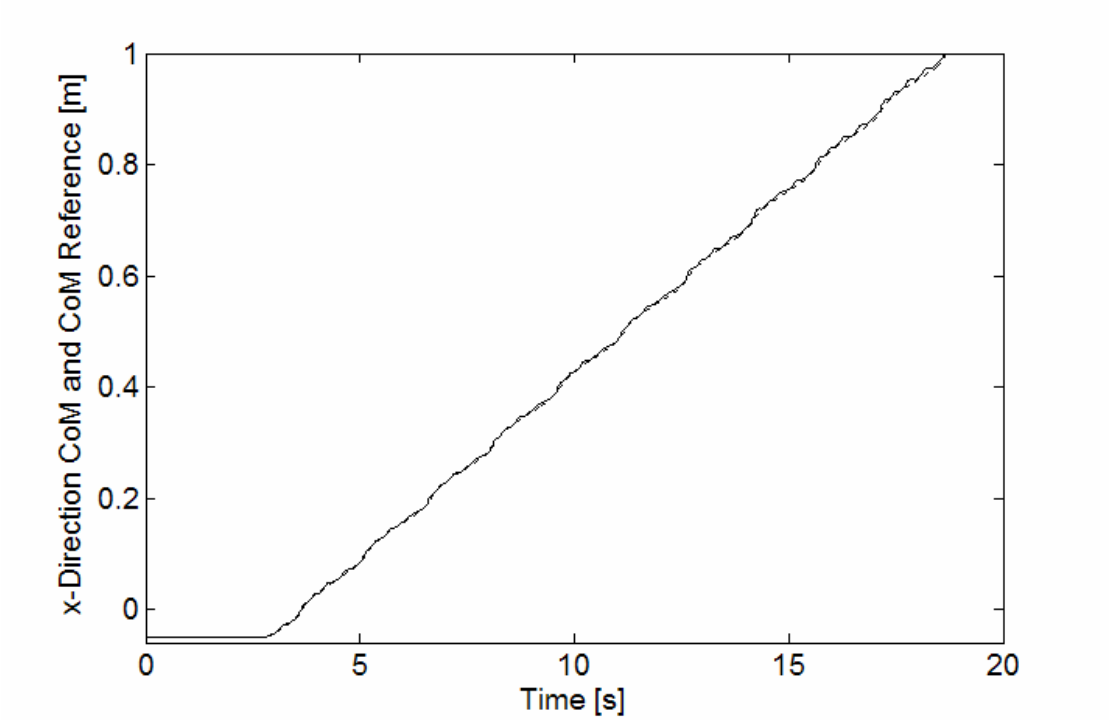

Figure 6.5 CMB position and CMB reference position x-direction curves with the one-mass-two-mass switching LIPM. The actual curve is plotted solid. Dotted curve belongs to the reference CMB.

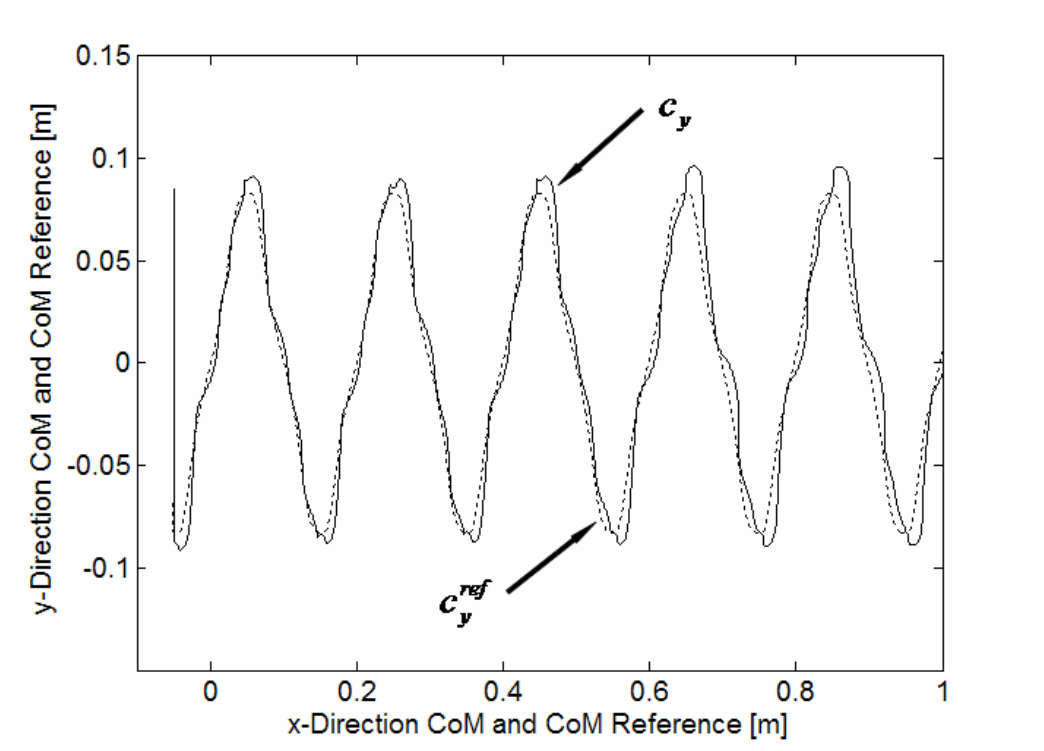

Figure 6.6 CMB position and CMB reference position projections on the *x*-*y*-plane (ground plane) with the one-mass-two-mass switching LIPM.

The integrals of the absolute deviations of the CMB trajectory from its references in the x-direction and y-direction are computed for the curves shown in Figure 6.3 and Figure 6.6. These errors are shown in Table 6.3

Table 6.3

Absolute Deviation Integrals

	x-direction	y-direction
One-mass model	0,0648	0,1449
Switching model	0,0577	0,0879

These results indicate that the tracking capability of the reference generated by the one-mass-two-mass switching model is achieved with a significantly better performance.

Chapter 7

7. CONCLUSION AND FUTUREWORK

A biped walking robot trajectory reference generation algorithm based on ZMP considerations and on the switching between one-mass and two-mass Linear Inverted Pendulum Models is presented in this thesis. State space descriptions of the inverted pendulum systems and offline simulations using these descriptions are employed to generate robot body center of mass reference trajcetories. The use of the two-mass linear inverted pendulum aims to constuct a satisfactorily detailed and yet simple enough model to be implemented for the minimization of the swing leg effects.

Simulation studies indicate a better performance of the model switching between one-mass and two-mass modes, compared with the one-mass LIPM case. This shows that the proposed method is a good candidate for implementations. Work on building a full-body robot for experimental validation is in continuation at Sabanci University.

It should be noted that no feedback from body configuration and ground contact forces is used during the walk. This also remains as a future work. It is interesting, however, to note that open loop controllers with well planned trajectories can provide steady and stable walking results. This suggests that a mixture of open loop control and corrective actions with online feedback information can generate robust walking algorithms.

Chapter 8

8. APPENDIX

In Figure (#), a full-state feedback system is shown. The command matrix N_x, that defines the desired value of the state, x_r. We wish to find N_x, so that some system output, $y_r = H_r x$ is at a desired reference value. N_u is a feedforward matrix for zero steady state error.

The feed forward gain, $\overline{N}$ which consists of N_x and N_u, can be computed so that no steady state error exists. Its value based on computing the steady state value of the control, u_{ss}, and the steady state values of the state, x_{ss}, that result in no steady state error, e.

If the system is Type 1 or higher, the steady state value of control for a step will be zero, and the solution will simply give us $N_u = 0$ and N_x, which defines the desired value of the state x.

The steady state requirements for the system are as follows.

$$u_{ss} = N_u r \tag{8.1}$$

$$N_x r = x_r = x_{ss} \tag{8.2}$$

$$H_r x_{ss} = y_r = r \tag{8.3}$$

where $H_r = [1 \quad 0 \quad 0 \quad 0]$.

Then, the system reduces to,

$$H_r N_x r = r \text{ and } H_r N_x = I \tag{8.4}$$

Furthermore in steady state we obtain

$$x(k+1) = \Phi x(k) + \Gamma u(k) \Rightarrow x_{ss} = \Phi x_{ss} + \Gamma u_{ss} \tag{8.5}$$

or

$$(\Phi - I)x_{ss} + \Gamma u_{ss} = 0 \tag{8.6}$$

By using the equations (8.1), (8.2) and (8.3) we get

$$(\Phi - I)N_x r + \Gamma N_u r = 0 \tag{8.7}$$

which reduces to

$$(\Phi - I)N_x + \Gamma N_u = 0 \tag{8.8}$$

System can be put into the following augmented form by using (8.4) and (8.8)

$$\begin{bmatrix} \Phi - I & \Gamma \\ H_r & 0 \end{bmatrix} \begin{bmatrix} N_x \\ N_u \end{bmatrix} = \begin{bmatrix} 0 \\ I \end{bmatrix} \tag{8.9}$$

The desired results are follows then as

$$\begin{bmatrix} N_x \\ N_u \end{bmatrix} = \begin{bmatrix} \Phi - I & \Gamma \\ H_r & 0 \end{bmatrix}^{-1} \begin{bmatrix} 0 \\ I \end{bmatrix} \tag{8.10}$$

REFERENCES

[1] www.answers.comtopiccore-anatomy

[2] Park, J. H. ,Kim, K. D., "Biped Robot Walking Using Gravity-Compensated Inverted Pendulum Mode and Computed Torque Control", *Proceedings of the 1998 IEEE International Conference on Robotics & Automation, pp. 3528-3533*, Leuven, Belgium, May 1998.

[3] Wollherr, D., "Design and Control Aspects of Humanoid Walking Robots", Thesis (PhD), Lehrstuhl für Steuerungs- und RegelungstechnikTechnische Universität München, Mar 2005.

[4] Marchese, S., Muscato, G. and Virk, G.S., "Dynamically Stable Trajectory Synthesis for a Biped Robot during the Single-Support Phase", *IEEUASME International Conference on Advanced Intelligent Mechatronics Proceedings,* Como, Italy, July 2001.

[5] Zhu, C., Tomizawa, Y., Luo, X. and Kawamura, A., "Biped Walking with Variable ZMP, Frictional Constraint, and Inverted Pendulum Model", *Proceedings of the 2004 IEEE International Conference on Robotics and Biomimetics*, Shenyang, China, August 2004.

[6] Vukobratovic, M., Borovac, B., Surla, D. and Stokic, "Biped Locomotion: Dynamics, Stability and Application", Springer, Verlag, 1990.

[7] Vukobratovic, M., BELGRADE SCHOOL OF ROBOTICS UDC 007.52(497.11)(045), The scientific journal FACTA UNIVERSITATIS, Series: Mechanics, Automatic Control and Robotics Vol.2, No 10, pp. 1349 – 1376, 2000.

[8] Sardain, P. and Bessonnet, G., "Forces Acting on a Biped Robot. Center of Pressure—Zero Moment Point", *IEEE Transactions on Systems, Man and Cybernetics—Part A: Systems and Humans, Vol. 34, NO. 5*, pp. 630-637, SEPTEMBER 2004.

[9] Flippo, D. K., "Design and Control of A Biped Robot", Thesis (MS), Department of Mechanical Engineering and the faculty of the graduate school of Wichita State University, 2004.

[10] Choong, E., Chew, C., Poo, A., Hong, G., "Mechanical Design of An Antropomorphic Bipedal Robot", *First Humanoid, Nanotechnology, Information Technology, Communication and Control Environment and Management (HNICEM) International Conference*, Manila, Philippines, 2003

[11] Hirai, K., Honda R&D Co. Ltd. Wako Research Center, "Current and Future Perspective of Honda Humanoid Robot", *Proceedings of the IEEE/RSJ International Conference on Intelligent Robots and Systems,* pp. 500-508, 1997.

[12] Espiau, B., Sardain, P., "The Anthropomorphic Biped Robot BIP2000", *Proceedings of the IEEE International Conference on Robotics & Automation*, pp. 3996-4001, San Francisco, April 2000.

[13] Kanehiro, F., Inaba, M., Inoue, H., "Development of a Two-Armed Bipedal Robot that can Walk and Carry Objects", *Proceedings of the IEEE/RSJ International Conference on Intelligent Robots and Systems,* pp. 23-28, 1996.

[14] www.humanoid.waseda.ac.jpbookletkato_2.html

[15] Raibert, M., "Legged Robots That Balance", MIT Press, Cambridge, MA, 1986

[16] Takanishi, A., Ogura Y. and Itoh, K., "Some Issues in Humanoid Robot Design"

[17] Yamaguchi, J., Soga, E , Inoue S. and Takanishi, A., "Development of a Bipedal Humanoid Robot - Control Method of Whole Body Cooperative Dynamic Biped Walking", *Proceedings of the 1999 EEE International Conference on Robotics & Automation,* pp. 368-374, Detroit, Michigan, May 1999.

[18] Nishiwaki, V., Sugihara, T., Kagami, S., Kanehiro, F., Inaba, M., Inoue, H., "Design and Development of Research Platform for Perception-Action Integration in Humanoid Robot : H6", *Proceedings of the 2000 IEEE/RSJ International Conference on Intelligent Robots and Systems,* pp. 1559-1564, 2000.

[19] Gienger, M.., Loffler, K., Pfeiffer, F., "Towards the Design of a Biped Jogging Robot", *Proceedings of the IEEE International Conference on Robotics & Automation,* pp. 4140-4145, Seoul, Korea, May 2001.

[20] Kim, J., Park, I., Lee, J., Kim, M., Cho B. and Oh, J., "System Design and Dynamic Walking of Humanoid Robot KHR-2", *Proceedings of the 2005 IEEE International Conference on Robotics and Automation*, pp. 1443-1448, Barcelona, Spain, April 2005.

[21] Yamasaki, F., Matsui, T., Miyashita, T. and Kitano, H., "PINO The Humanoid that Walk",

[22] Kuroki, Y., Digital Creatures Laboratory Sony Corporation, "A Small Biped Entertainment Robot",

[23] Ishida, T., Kuroki, Y., Yamaguchi, J., Fujita, M., Doi, T., "Motion Entertainment by a Small Humanoid Robot Bsed on OPEN-R", *Proceedings of the IEEE/RSJ International Conference on Intelligent Robots and Systems,* pp. 1079-1086, 2001.

[24] Kaneko, K., Kajita, S., Kanehiro, F., Yokoi, K., Fujiwara, K., Hirukawa, H., Kawasaki, T., Hirata, M. and Isozumi, T., "Design of Advanced Leg Module for Humanoid Robotics Project of METI" *Proc. IEEE Int. Conference on Robotics and Automation*, pp. 38-45, 2002.

[25] Kaneko, K., Kajita, S., Kanehiro, F., Yokoi, K., Fujiwara, K., Hirukawa, H., Kawasaki, T., Hirata, M. and Isozumi, T., "Design of Prototype Humanoid Robotics Platform for HRP", *Proceedings of the 2002 IEEE/RSJ Intl. Conference on Intelligent Robots and Systems EPFL*, pp. 2431-2436, Lausanne, Switzerland, October 2002.

[26] Akachi, K., Kaneko, K., Kanehira, N., Ota, S., Miyamori, G., Hirata, M., Kajita, S. and Kanehiro, F., "Development of Humanoid Robot HRP-3P", *Proceedings of 2005 5th IEEE-RAS International Conference on Humanoid Robots,* pp. 50-55, 2005.

[27] Hyon, S., Cheng, G., "Passivity-Based Full-Body Force Control for Humanoids and Application to Dynamic Balancing and Locomotion", *Proceedings of the 2006 IEEE/RSJ International Conference on Intelligent Robots and Systems,* rr. 4915-4922, Beijing, China, October 2006.

[28] S. Hyon and G. Cheng, "Gravity Compensation and Full-Body Balancing for Humanoid Robots," *IEEE-RAS/RSJ International Conference on Humanoid Robots (Humanoids 2006)*, CD-ROM, pp. 214-221, Dec. 2006.

[29] www.sarcos.comhighperf_videos.html

[30] Hirai, K., Hirose, M., Haikawa, Y., Takenaka, T., "The Development of Honda Humaonid Robot", *Proc. IEEE Int. Conference on Robotics and Automation*, pp. 1321-1326, May 1998.

[31] Huang, Q., Kajita, S., Koyachi, N., Kaneko, K., Yokoi, K., Arai, H., Komoriya, K. and Tane, K., "A High Stability, Smooth Walking Pattern for a Biped. Robot", *Proceedings of the 1999 IEEE International Conference on Robotics & Automation,* pp. 65-71, Detroit, Michigan, May 1999.

[32] Kajita, S., Matsumoto, O. and Saigo, M., "Real-time 3D walking pattern generation for a biped robot with telescopic legs", *Proceedings of the 2001 IEEE International Conference on Robotics & Automation*, pp. 2299-2306, Seoul, Korea, May 2001.

[33] Kajita, K., Tani, K., "Study of Dynamic Biped Locomotion on Rugged TerrainTheory and Basic Experiment", *Proceedings of 94 Int. Conf. on Advanced Robotics*, pp. 741-746, 1994.

[34] Kajita, S., Kanehiro, F., Kaneko, K., Fujiwara, K., Harada, K., Yokoi, K., Hirukawa, H., "Biped Walking Pattern Generation by using Preview Control of Zero-Moment Point",

In Proceedings of the 2003 IEEE International Conference on Robotics& Automation, pp. 1620-1626, Taiwan, 2003.

[35] Kajita, S., Kaneko, K., Harada, K., Kanehiro, F., Fujiwara, K., "Biped Walking on a Low Friction Floor, In Proceedings of 2003 IEEE/RSJ International Conference on Intelligent Robots and Systems, 2004, pp. 3546-3552, Sendai, Japan, 2004.

[36] Kanehira, N., Kawasaki, T., Ohta, S., Isozumi, T., Kawada, T., Kanehiro, F., Kajita, S. and Kaneko, K., "Design and Experiments of Advanced Leg Module (HRP-2L) for Humanoid Robot (HRP-2) Development", *Proceedings of the 2002 IEEE/RSJ Intl. Conference on Intelligent Robots and Systems EPFL*, pp. 2455-2460, Lausanne, Switzerland, October 2002.

[37] Lohmeier, S., Lijffler, K., Gienger, M., Ulbrich, H., Pfeiffer, H., "Computer System and Control of Biped "Johnnie" ", *Proceedings of the 2004 IEEE International Conference on Robotics & Automation*, pp. 4222-4227, New Orleans, LA, April 2004.

[38] Sugihara, T., Nakamura, Y., Inoue, H., "Realtime Humanoid Motion Generat ion through ZMP Manipulation based on Inverted Pendulum Control", *Proceedings of the 2002 IEEE International Conference on Robotics & Automation*, pp. 1404-1409, Washington, DC, May 2002.

[39] K. Erbatur, A. Okazaki, K. Obiya, T. Takahashi and A. Kawamura, "A study on the zero moment point measurement for biped walking robots", *Proc. 7th International Workshop on Advanced Motion Control*, pp. 431-436, Maribor, Slovenia, 2002

[40] Nishiwaki, K., Nagasaka, K., Inaba, M. and Inoue, H., "Generation of Reactive Stepping Motion for a Humanoid by Dynamically Stable Mixture of Pre-designed Motions", *Proc. of the 1999 IEEE International Conference on Systems, Man, and Cybernetics*, pp.702-707, Tokyo Japan, 1999.

[41] Kajita, S., Morisawa, M., Harada, K., Kaneko, K., Kanehiro, F., Fujiwara, K. and Hirukawa, H., "Biped Walking Pattern Generator allowing Auxiliary ZMP Control," *Proc. of 2006 IEEE/RSJ Int. Conf. on Intelligent Robots and Systems*, pp.2993-2999, 2006.

[42] Spong, M., Vidyasagar, M., “Robot Dynamics and Control”, John Wiley and Sons, 1989.

[43] R. Featherstone, *Robot Dynamics Algorithms*, Kluwer Academic Publishers, 2003

[44] Ayhan, O. and K. Erbatur, “Biped Walking Robot Hybrid Control with Gravity Compensation,” *Proc. Int. Conf. on Industrial Electronics, Control and Instrumentation, IECON 2005*, Raleigh, USA,2005

[45] Fujimoto, Y., A. Kawamura, “Simulation of an Autonomous Biped Walking Robot Including Environmental Force Interaction”, *IEEE Robotics and Automation Magazine, pp. 33-42,* June 1998

[46] Erbatur, K. and A. Kawamura, “A New Penalty Based Contact Modeling and Dynamics Simulation Method as Applied to Biped Walking Robots," *Proc. 2003 FIRA World Congress*, October 1-3, 2003 Vienna, Austria

[47] Kurt, O. and K. Erbatur, “Biped Robot Reference Generation with Natural ZMP Trajectories”, Proc. The 9th IEEE International Workshop on Advanced Motion Control, AMC 2006, Istanbul, Turkey

[48] Franklin, G.F., Powell, J.D., Workman, M., “Digital Control of Dynamic Systems”, Addison Wesley Longman, 1998

[49] K. Erbatur and U. Seven, “Humanoid Gait Synthesis with Moving Single Support Zmp Trajecories”, accepted for publication in *Proc. The 13th IASTED International Conference on Robotics and Applications RA 2007,* Würzburg, Germany, August, 2007